DOKUZ EYLÜL UNIVERSITY
GRADUATE SCHOOL OF NATURAL AND APPLIED SCIENCES

NUMERICAL AND EXPERIMENTAL INVESTIGATION OF HOUSEHOLD REFRIGERATORS WITH VACUUM COMPARTMENT

by
İsmail Çağlar EBEPERİ

April, 2021
İZMİR

NUMERICAL AND EXPERIMENTAL INVESTIGATION OF HOUSEHOLD REFRIGERATORS WITH VACUUM COMPARTMENT

A Thesis Submitted to the
Graduate School of Natural and Applied Sciences of Dokuz Eylül University
In Partial Fulfilment of the Requirements for the Degree of Master of Science
in Mechanical Engineering, Energy Program

by
İsmail Çağlar EBEPERİ

April, 2021
İZMİR

M.Sc THESIS EXAMINATION RESULT FORM

We have read the thesis entitled **"NUMERICAL AND EXPERIMENTAL INVESTIGATION OF HOUSEHOLD REFRIGERATORS WITH VACUUM COMPARTMENT"** completed by **İSMAİL ÇAĞLAR EBEPERİ** under supervision of **PROF. DR. DİLEK KUMLUTAŞ** and we certify that in our opinion it is fully adequate, in scope and in quality, as a thesis for the degree of Master of Science.

Prof. Dr. Dilek KUMLUTAŞ

Supervisor

Prof. Dr. Can Özgür ÇOLPAN

(Jury Member)

Doç. Dr. Mustafa Turhan ÇOBAN

(Jury Member)

Prof.Dr. Özgür ÖZÇELİK

Director

Graduate School of Natural and Applied Sciences

ACKNOWLEDGEMENTS

First of all, I would like to thank my advisor Prof. Dr Dilek KUMLUTAŞ for her unwavering guidance and her profound belief in my work throughout the thesis.

I would like to especially thank my associate and my dear old friend Özgün ÖZER for his mental and scientific support. Without his motivation and hard work, this thesis cannot be accomplished.

I would like to present my sincere gratitude to Research Assistant Utku Alp YÜCEKAYA for sharing his knowledge and help.

I would like to thank my colleagues in Vestel Home Appliances Company for their help and support for the experimental studies.

Finally, I would like to gratefully thank my wife Özge EBEPERİ and my family for their patience and unconditional support in every part of my life.

İsmail Çağlar EBEPERİ

NUMERICAL AND EXPERIMENTAL INVESTIGATION OF HOUSEHOLD REFRIGERATORS WITH VACUUM COMPARTMENT

ABSTRACT

One of the effective methods in the literature for increasing food storage time is to decrease the pressure in the section. When the vacuum chamber is implemented in household refrigerators, the forced convection cannot be used for chilling food. Therefore, the system's thermal design needs to be reconsidered to chill the food in the right condition. This study includes the design, numerical, and experimental studies of the vacuum compartment system designed for household refrigerators.

In this study's system design section, the design parameters, operating principle, and selection methods of the components used for the vacuum compartment are explained. Numerical calculation methods are used to decide on the determined design parameters and the aerodynamic structure of the system. Computational fluid dynamics principles are used as the numerical calculation method. Eight different design points, including various models and different boundary conditions, were calculated. Due considering these calculations, the ideal system design was decided.

For the concept validation, the prototype was tested by observing the thermal behaviour of the system. The results of the experiments are compared with the numerical study results. The numerical calculation method used for the parameter selections decided for system design has been verified.

The main targeted effect of the vacuum system in household refrigerators is the effect on food storage times. With the experimental studies carried out in this study, it has been observed that the system concept significantly increases the food storage times.

Keywords: Household refrigerator, vacuum cooling, vacuum chamber, computational fluid dynamics, CFD, food shelf life

VAKUM BÖLMELİ EV TİPİ BUZDOLAPLARININ NÜMERİK VE DENEYSEL İNCELENMESİ

ÖZ

Gıda saklama süresini belirleyen en önemli faktörlerden biri, gıdaları doğru koşullar altında saklamaktır. Vakum sistemi, evdeki buzdolaplarına uygulandığında, buzdolabının havası, vakum bölmesindeki yiyeceklere doğrudan temas etmediğinden zorlanmış taşınım yiyeceklerin soğutulması için kullanılamaz. Bu sebeple yiyeceklerin doğru koşulda soğutulması için sistemin ısıl tasarımının yeniden gözden geçirilmesi gerekmektedir. Bu çalışma, ev tipi buzdolapları için tasarlanan vakum bölmesi sisteminin tasarım, sayısal ve deneysel çalışmalarını içermektedir.

Bu çalışmanın sistem tasarımı bölümünde ev tipi buzdolabına entegre edilecek vakum sisteminin tasarım parametreleri, çalışma prensibi ve kullanılan komponentlerin seçim metotları anlatılmaktadır. Belirlenen tasarım parametrelerine ve sistemin aerodinamik yapısına karar vermek için hesaplamalı akışkanlar dinamiği ilkeleri sayısal hesaplama yöntemi olarak kullanılmıştır. Farklı modeller ve farklı sınır koşulları içeren 8 farklı tasarım sonucu hesaplanarak ideal sistem tasarımına karar verilmiştir.

Çalışmanın deneysel bölümünde vakum bölmesi konseptinin doğrulanması için tasarlanan prototip, sistemin termal davranışı gözlemek adına test edildi. Yapılan deney sonuçları sayısal çalışma sonuçlarıyla karşılaştırıldığında, sistem tasarımı için karar verilen parametre seçimlerinde kullanılan sayısal hesaplama yöntemi doğrulanmıştır.

Ev tipi buzdolaplarına vakum sisteminin entegre edilmesi konseptinin asıl hedeflenen etkisi ise gıdaların saklama sürelerine olan etkisidir. Bu çalışmada yapılan deneysel çalışmalar ile sistem konseptin gıda saklama sürelerini önemli ölçüde arttırdığı görülmüştür.

Anahtar kelimeler: Ev tipi buzdolabı, vakumlu soğutma, vakum bölmesi, hesaplamalı akışkanlar dinamiği, gıda raf ömrü

CONTENTS

Page

LIST OF FIGURES

Page

LIST OF TABLES

Page

CHAPTER 1
INTRODUCTION

Preservation of food is one of the most extensive applications in refrigeration. Without modern refrigerators, the packing industry, transportation of foods, and preparation of many edibles would not be only challenging but, in many cases, almost impossible. Modern refrigeration technologies save large quantities of fish, milk, eggs, meat etc. from spoilage (Miller et al., 2004).

A significant amount of food goes to waste without consuming due to purchasing excessive food and food storage time due to its variability. One of the most crucial factors determining food storage time is keeping food under the right conditions. Although suitable temperatures are provided in household refrigerators, it is insufficient to extend maximum food storage time. In addition to providing proper storage conditions (temperature, humidity, etc.), one of the effective methods in the literature for increasing food storage time is to prevent aerobic bacteria's growth by discharging some of the air in the section the food is stored.

This thesis included the design, experiment, and validation stages of the vacuum compartment for a household refrigerator, aiming to extend the food storage time by optimizing the pressure, humidity, and temperature parameters of a particular compartment in the refrigerator.

1.1 Refrigeration

Refrigeration is the process by which the heat is removed from either a substance or space. This heat removal causes the substance or space to become cool (Miller et al., 2004). From a thermodynamical point of view, refrigeration is the heat transfer from a low-temperature territory to a high-temperature one (Çengel et al., 2018).

The second law of thermodynamics shows that the work input is also required for the heat transfer between the low and the high-temperature zones. This work input is accomplished by a refrigerator, which is a cyclic machine. Refrigerants are used in the cycle as the working fluids (Çengel et al., 2018).

1.1.1 The Ideal Refrigeration Cycle

The refrigeration cycles are thermodynamic cycles on which the refrigerator operates. In the literature, one of the three well-known refrigeration cycles, the first one is the reversed Carnot cycle, the second one is the vapour-compression refrigeration cycle, and the final one is the gas refrigeration cycle (so-called the reversed Brayton cycle). In addition to these primary refrigeration cycles, modified refrigeration systems can be obtained, such as absorption refrigeration, cascade refrigeration, and steam jet refrigeration systems (Çengel et al., 2018). Furthermore, some systems in which the refrigerants are not used include thermoelectric, thermoacoustic, and magnetic systems (Dinçer & Kanoglu, 2010).

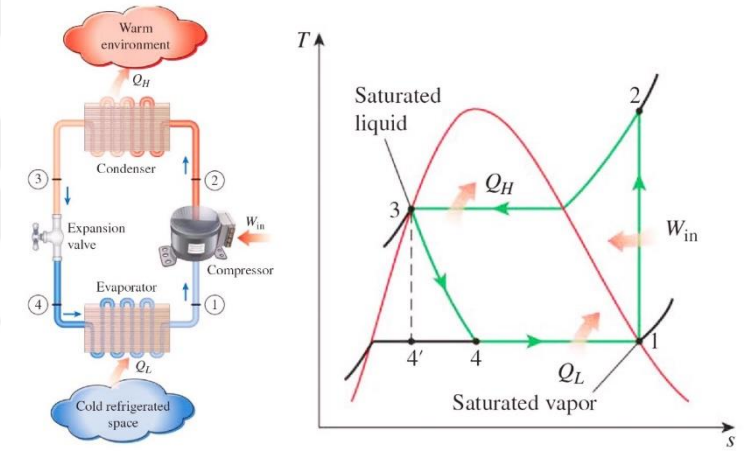

Figure 1.1 Schematic and T-S diagram for the ideal refrigeration cycle (Çengel et al., 2018)

In household refrigerators, the most widely used refrigeration systems are vapour-compression systems that consist of a compressor. In Figure 1.1, an ideal vapour-compression refrigeration cycle is depicted. In addition to household refrigerators, the air-conditioning systems and heat pumps use this cycle (Çengel et al., 2018).

The vapour-compression refrigeration cycle comprises of four steps:

- 1-2 Isentropic compression
- 2-3 Heat rejection at constant-pressure
- 3-4 Throttling
- 4-1 Heat absorption at constant-pressure

At state 1, the refrigerant in the form of saturated vapour enters the compressor. Then it is compressed to the condenser pressure while the refrigerant temperature increases significantly. As a result, the refrigerant is transformed into the state of superheated vapour when entering the condenser at state 2. At state 3, it becomes a saturated liquid while losing heat. At this state, the refrigerant temperature continues to be higher compared to the medium. The refrigerant passes through an expansion valve until it reduces to the evaporator pressure. During this pressure drop, the temperature of the refrigerant also reduces to below the medium temperature. So, the refrigerant in the form of saturated mixture enters the evaporator at state 4. It absorbs heat and evaporates. The refrigerant leaving the evaporator is a saturated vapour. It re-enters the compressor, and the cycle is completed.

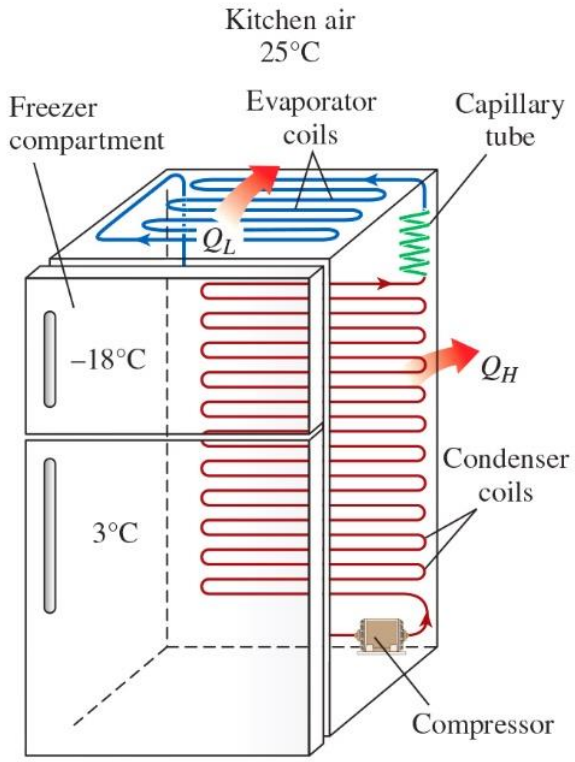

Figure 1.2 An ordinary household refrigerator (Çengel et al., 2018)

In the case of a household refrigerator, as shown in Figure 1.2, the evaporator refers to the heat transferring tubes in the freezer where the refrigerant absorbs the heat. In contrast, the condenser refers to the coils behind the refrigerator, where the heat is dispersed to the surrounding.

Based on the T-s diagram in Figure 1.1, the area under the curve refers to the heat transfer for reversible processes. Among the specified areas under the curve, the process curve 4-1 refers to the heat absorbed in the evaporator, whereas the process curve 2-3 refers to the heat released in the condenser. As the evaporating temperature increases or the condensing temperature is reduced, the COP is improved by %2 to %4, correspondings to each °C change (Çengel et al., 2018).

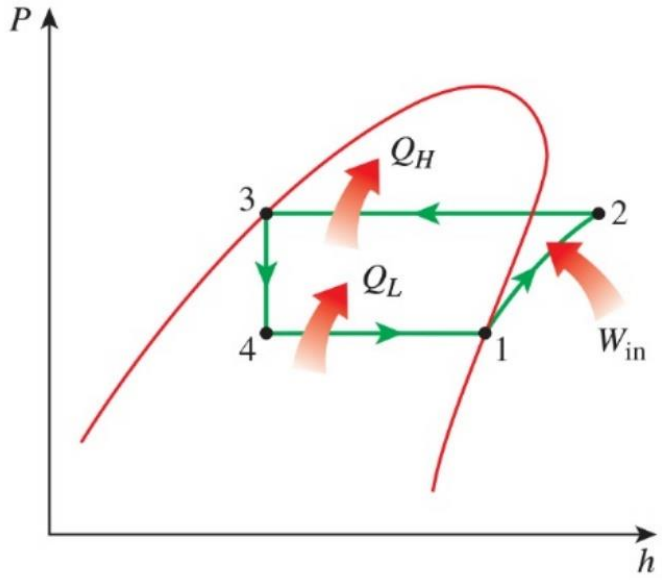

Figure 1.3 The P-h diagram of ideal vapour-compression refrigeration (Çengel et al., 2018)

In addition to the T-s diagram, the P-h diagram is often used to analyze vapour-compression refrigeration cycles, as depicted in Figure 1.3. On this diagram, there are three straight lines whose lengths are proportional to the heat transfer from the evaporator and the condenser. The ideal vapour-compression refrigeration cycle consists of an irreversible throttling process which offers a more realistic model for the actual vapour-compression refrigeration cycle. If there were an isentropic turbine instead of a driving mechanism, the refrigerant's access to point to evaporator shifts 4' from 4 in Figure 1.1, which decreases the system input. However, instead of the expansion valve, the turbine cannot find practical use because of the cost-up and complexity. All four components are steady-flow devices, and the related process cycles can be analyzed as steady-flow processes. The refrigerant's kinetic and potential energy changes are neglected because they are relatively small compared to the work

and heat transfer terms. Then the steady-flow energy equation on a unit-mass basis is simply as below:

$$(q_{in} - q_{out}) + (w_{in} - w_{out}) = h_e - h \tag{1.1}$$

The condenser and the evaporator do not contribute to the work, and the compressor can be taken as adiabatic. Overall, the COPs of refrigerators and heat pumps comprising the vapour-compression refrigeration cycle can be shown as below:

$$COP_R = \frac{q_L}{W_{net,in}} = \frac{h_1 - h_4}{h_2 - h_1} \tag{1.2}$$

$$COP_{HP} = \frac{q_H}{W_{net,in}} = \frac{h_2 - h_3}{h_2 - h_1} \tag{1.3}$$

where $h_1 = h_{g@P1}$ *and* $h_3 = h_{g@P3}$ for the ideal case (Çengel et al., 2018).

1.1.2 Actual Refrigeration Cycle

There are fundamental differences between actual refrigeration and an ideal cycle. Mostly the differences are due to the irreversibilities that occur in various components. Two well-known causes of irreversibilities are fluid friction that causes pressure drops and heat transfer to or from the surrounding medium. The T-s diagram of an actual refrigeration cycle can be depicted as in Figure 1.4.

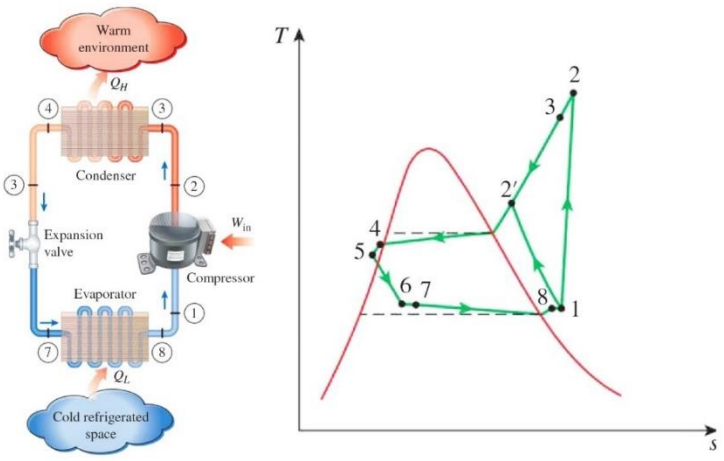

Figure 1.4 The schematic and T-s diagram for the actual refrigeration cycle (Çengel et al., 2018)

In the case of an ideal cycle, the refrigerant's physical state leaving the evaporator and entering the compressor is a saturated vapour. Nevertheless, it may not be so obvious to obtain the saturated vapour in lack of precise control. Thus, it is far more plausible to design the system with a slightly superheated refrigerant at the compressor inlet. Via this acceptance, it ensures that the refrigerant is vaporized when it passes through the compressor. Additionally, the linkage between the evaporator and the compressor is so long that the pressure drop and heat transfer from the surroundings cannot be neglected. The superheating, heat absorbance, and pressure drops cause the specific volume to increase and the power input to the compressor to increase as well.

When the ideal cycle is further examined, it is seen that the compression process is internally reversible and adiabatic, isentropic as well. However, the actual compression process involves frictional effects and heat transfer, as discussed. These two effects may have an adverse effect on entropy. For instance, the entropy is increased by friction and increased or decreased by heat transfer depending on the direction. Based on the domination of effects, either the entropy of the refrigerant may increase or decrease in the case of an actual compression process. In the compression process 1-2′, the refrigerant's specific volume and the work input requirements are smaller. Thus, this process may be more desirable compared to the isentropic compression process. In conclusion, if it is more practical and economical, it is more plausible to let the refrigerant to be cooled during this process.

As we continue on the ideal case, the refrigerant's physical state is assumed as a saturated liquid after leaving the condenser. In an actual situation, there is again a pressure drop in the condenser and the linkage between the condenser and the compressor and the throttling valve. Similarly, it is not exact to have the refrigerant as a saturated liquid. So, it is not desired to transfer the refrigerant to the throttling valve until it is fully condensed. Thus, the refrigerant is subcooled beforehand with a lower enthalpy that may cause it to absorb more heat from the refrigerated space. In the end, it is an unwanted situation (Çengel et al., 2018).

1.2 Household Refrigerator

A household refrigerator is known as a cyclic machine having the food storage function and keeping them fresh for a long time. These devices are also referred to as "refrigerating appliances" in the standard of ISO15502. They are defined as an insulated cabinet, cooled by natural convection or a frost-free system (ISO 15502 (International Organization for Standardization 15502), 2005). According to this definition, the main properties of household refrigerators are discussed in the next subsections.

1.2.1 Insulated Cabinet

A household refrigerator contains an insulated cabinet that sustains a low-temperature medium for foods compared to the surrounding conditions for a long period. It is well-known that the heat is transferred from higher to lower temperature. From this point of view, it is obvious that there is continuous heat gain inside the household refrigerator because of the household refrigerator's lower inner temperature. Thus, to eliminate this heat gain, the household refrigerator's most crucial component is the insulated cabinet. Additionally, the insulating cabinet serves as structural support in terms of strength to the household refrigerator. In the cabinet design, several aspects are included in terms of strength, such as the weight of shelves, foods, pieces of equipment, and loads caused by either shipping or daily usage.

Insulated cabinets comprise three layers, including an inner plastic generally made up of a single plastic sheet High Impact Polystyrene (HIPS), an outer shell made up of structural steel sheet metal and foam of polyurethane as an insulation material in the middle. (American Society of Heating & Air-Conditioning, 2006).

1.2.2 Compartments

In the design of household refrigerators, different compartments may occur based on the types of foods. Therefore, each compartment has to be specialized in terms of environmental conditions to sustain the storage conditions of foods to be stored in it. Commonly, the household refrigerators have essential compartments for fresh-food storage, freezer, eggs and vegetables. Specifically, some cellar compartments may be

either warmer or colder than the fresh-food compartment depending on the foodstuffs (ISO 15502 (International Organization for Standardization 15502), 2005). Furthermore, more specific compartments for meat or fish storage may be designed in the household refrigerators (American Society of Heating & Air-Conditioning, 2006).

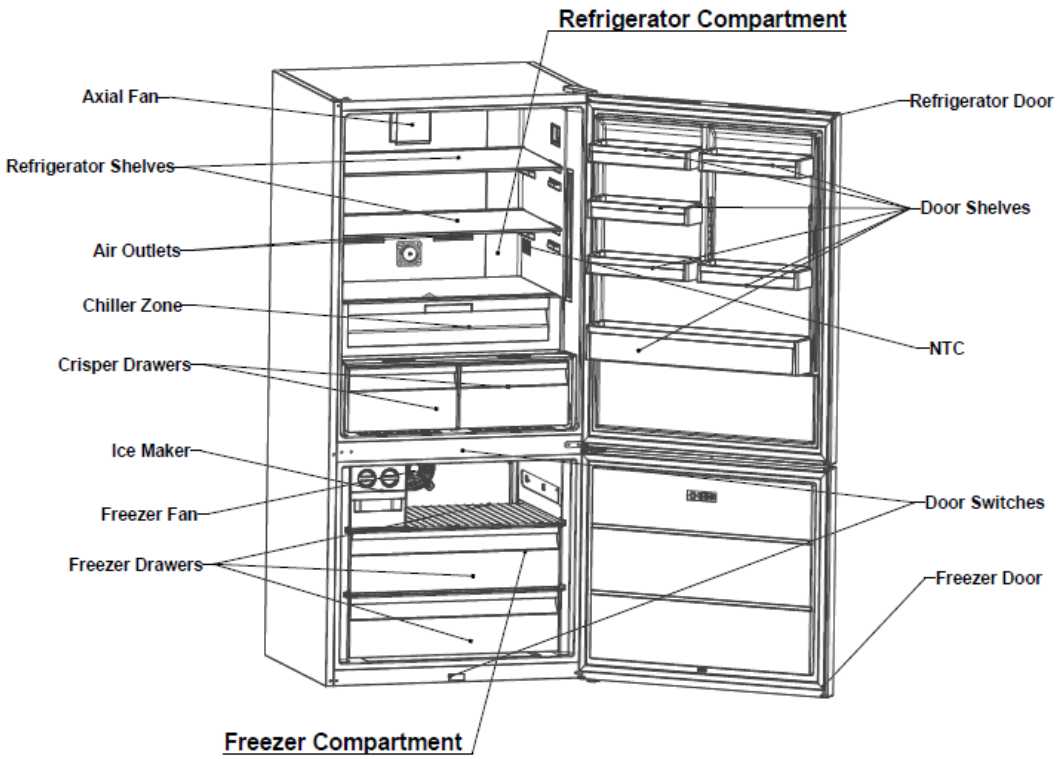

Figure 1.5 Compartments of a household refrigerator

Figure 1.5 shows the compartments of a refrigerator with a bottom freezer. As shown in Figure 1.5 refrigerator compartment has different zones with different temperatures. Crisper drawers are fresh food compartments like vegetables and fruits. The chiller zone is used for meats and delicatessen products that need a colder space than fresh foods. For that reason, the chiller zone is the coldest place in the refrigerator compartment.

1.2.3 Inner Environment Conditions

It is crucial in compartment design that the volume should be suitable to inhibit the microorganisms responsible for the decay of foods. There are many factors in microorganism growth in food, such as food characteristics in terms of chemical

structure, pH, inhibitors, and environmental conditions in terms of temperature and relative humidity (Çengel et al., 2018). Thus, the primary purpose is to sustain the environmental conditions of compartments at the desired levels.

The storage life of fresh foods can be differentiated under different environmental conditions. For instance, between 1 and 4 C temperature is enough for red or white meat, vegetables to be stored for a couple of days. If it is desired to store the foods for several months, they should be kept between -18 °C and -35 °C. Specifically, for most fruits and vegetables, the optimum storage temperature is about 0.5 to 1 C. Nevertheless, some of them go through irreversible physical changes. For instance, when bananas and cucumbers are kept between 0 and 10 C, unwanted physiological changes can be observed (Çengel et al., 2018).

1.3 Vacuum Cooling

Concerning some specific foods and particularly vegetables, a quick evaporative cooling application can be conducted, known as vacuum cooling. Some food manufacturers use this technology concerning competitiveness, product safety and quality. This technology's advantages can be listed as shorter processing times, consequent energy savings, improved product shelf life, quality, and safety. However, its disadvantage is the limited range of applications. As a typical example, lettuce and mushrooms have been cooled under a vacuum, as well as there are some possible applications regarding meat and bakery products, fruits, and other vegetables (McDonald & Sun, 2000).

The critical point of vacuum cooling is quick moisture evaporation. When water within the products evaporates, it tends to absorb heat (so-called latent heat) required to reach a higher energy level at a gaseous state. This amount of latent heat must be supplied either from the product or from the medium. The evaporation of water starts directly dependent on the surrounding vapour pressure, as shown in Figure 1.6. At atmospheric pressure, the boiling of water starts at 100°C. If the pressure is reduced, the boiling point of water decreases. In a way, vacuum cooling can be depicted as the opposite process of pressure cooking (Sun & Zheng, 2006).

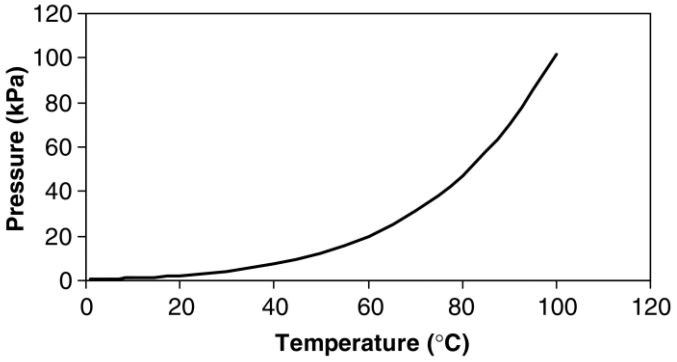

Figure 1.6 The relation between the saturated vapour pressure and saturated temperature (Sun & Zheng, 2006)

When placing a product in a closed vessel and reducing the pressure by a vacuum pump, the product's free water tends to evaporate. The latent heat in this evaporation process is gathered from the product's sensible heat as there is not any other medium than air. When the product releases heat, and its temperature is started to decrease, the cooling process is achieved in the end. With the evaporation process, a vapour is also generated, and it must be evacuated from the vessel immediately to slow down the cooling process. The temperature of the product can be settled to the desired degree by regulating the pressure of the medium in the final state. Desirably, it is set above 6.5 mbar in order not to damage the food's physical structure (McDonald et al., 2001).

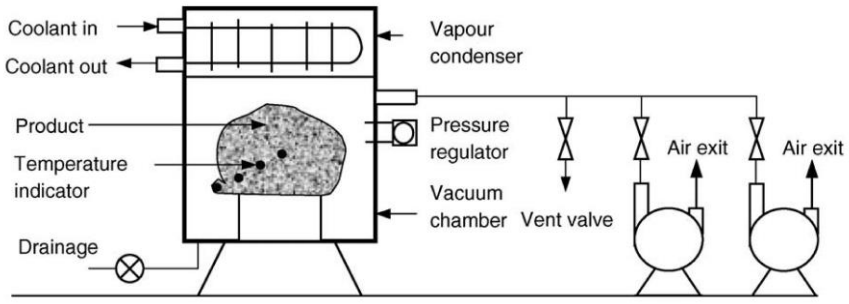

Figure 1.7 Layout of the vacuum cooling system (Sun & Zheng, 2006)

Vacuum cooling installation may have different size and shape, but the essential parts can be listed as a chamber, pump, and vapour condenser, as shown in Figure 1.7. The vacuum chamber can be described as where the food is set to be cooled and sealed (Sun & Zheng, 2006).

1.3.1 Mathematical Model Of Vacuum Cooling

According to Wang et al., the vacuum cooling process separates into two phases. The first phase comprises air removal in the chamber, while the second phase comprises the primary cooling process in the decreasing pressure (L. Wang & Sun, 2002).

The sum of the partial pressures of air and water vapour is the total pressure inside the chamber.

$$P_{vc} = P_a + P_v \tag{1.4}$$

According to Houška et al., the required speed of the vacuum pumps for a vacuum system is calculated by the evacuation time to the flash point (Houška et al., 1996).

$$S = \eta \frac{V_f}{t}_{fp} ln \frac{P_{atm}}{P_{fp}} \tag{1.5}$$

In equation 1-5, S is the pumping speed, and η is the vacuum pump's efficiency. V_f is the free volume of the vacuum chamber, t_{fp} is the time, and P_{fp} is the pressure of the flashpoint.

The mass flow rate of air can be determined as:

$$\dot{m}_{a,o} = S_{\rho a} \tag{1.6}$$

Air leakage is assumed to be adiabatic compressible flow through a nozzle, and its rate is determined by (Houška et al., 1996):

$$\dot{m}_{a,i} = A_i \left[\left(\frac{2\gamma}{\gamma - 1}\right)\left(\frac{P_{atm}^2 M_a}{RT_{K,vc}}\right)\right]^{0.5} \left[\left(\frac{P}{P_{atm}}\right)^{\frac{1+\gamma}{\gamma}} - \left(\frac{P}{P_{atm}}\right)^2\right]^{0.5} \tag{1.7}$$

where A_i is the leakage area.

The below equation determines the decrease rate of the air pressure:

$$\frac{dP_a}{dt} = -\frac{\dot{m}_{a,e} R T_{K,vc}}{M_a V_f} \tag{1.8}$$

The ideal gas equation can determine the vapour density.

From this relation, the mass flow rate of vapour can be shown as:

$$\dot{m}_{v,o} = S\rho_V \tag{1.9}$$

Therefore, the decrease of the total pressure can be expressed by,

$$\frac{dP}{dt} = \frac{dP_a}{dt} + \frac{dP_v}{dt} \tag{1.10}$$

1.3.2 Advantages and Disadvantages of Vacuum Cooling

Vacuum cooling has both advantages and disadvantages in the food industry. They are compared in Table 1.1. Among the advantages, the most crucial one is reducing product temperature in an enormously short period (Zheng & Sun, 2005). The cooling profiles of foods are given in Figure 1.8. It has been shown that the rate of vacuum cooling is 50% faster for meat (McDonald & Sun, 2000) as well as 60 times quicker for vegetables (L. Wang & Sun, 2002) compared to the conventional methods. Under the vacuum, the cooling rate of vegetables can reach 0.5°C/min. It is even enhanced up to 0.05–3°C/h in the case of cold storage. There are two ways to increase the cooling rate for the latter. It may be managed by either reducing the temperature or increasing the velocity of the medium. However, both of them may cause product damage because of freezing.

The main reason behind the distinguished cooling rates among vacuum and conventional methods is the key differences in the mechanisms. In the case of conventional methods, the successive steps are conductive and convective heat transfer. Conductive heat transfer occurs from the core to the surface and is the rate-limiting step because of lower thermal conductivity. Convective heat transfer occurs from the surface to the medium. On the contrary, the vacuum cooling step comprises water evaporation (Sun & Wang, 2000). Therefore, the rate is much faster, based on the 1:16 ratio (Sun, 2001). This beneficial fast cooling rate opens new opportunities

for vacuum cooling in the food industry, e.g. less time, enhanced production, lower energy (Chen, 1986), less microbial effects (Wang & Sun, 2002).

Table 1.1 Advantages and disadvantages of vacuum cooling (Sun & Zheng, 2006)

Product	**Advantages**	**Disadvantages**
Bakery	• Rapid cooling rate • Enhanced productivity • Enhanced product quality • Minimized weight loss	• Absence of volatile aromatic component • Specialized technology required
Meat	• Rapid cooling rate • Enhanced safety • Lower cost • Lower microbial growth	• Lower product yield • Absence of juicy and tender property
Fruits and vegetables	• Enhanced shelf-life • Short cooling time • Faster distribution • Moderating temperature • Lower cost • Homogeneous cooling	• Limited with leafy vegetables, mushrooms • Increased capital cost • Increased weight loss
Ready meals	• Integrated systems • Applicable for heat-sensitive foods	• Cleaning requirement • Safety concerns
Sauces, soups and others	• Applicable for liquid foods • Cooking and cooling at the same compartment • Moderating weight loss	• Difficulty in continuous process • Cleaning requirement

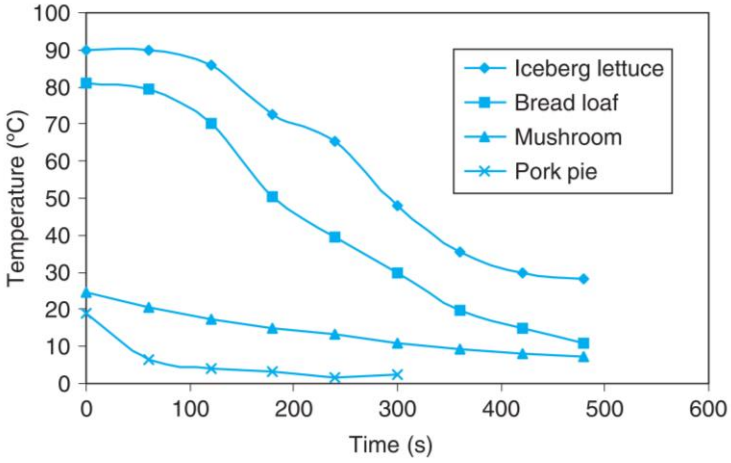

Figure 1.8 Cooling curves for some food products (Sun & Zheng, 2006)

In contrast to conventional cooling methods, water evaporation occurs in the core and on the surface under vacuum at the same time. Therefore, the product has a homogeneous internal temperature profile. Besides the product itself, a large number of products can be cooled at the same rate under vacuum cooling regardless of the position of the product in a pile (Malpas, 1972). Furthermore, large products have unified temperature distribution among the surface and core under vacuum compared to air blast (Sun & Wang, 2000) and water immersion (McDonald et al., 2001). The homogeneous temperature profile may be more useful in the food industry. For example, baked foods under vacuum are generally more potent because of less contraction (Acker & Ball, 1977; Chriastel, 1978; Shipman, 1978).

In the air blast and cold storage cooling, the rate is directly proportional to the surface area. For this reason, a larger storage surface area is needed to have a proper cooling process. This limitation is not included in vacuum cooling. As mentioned before, the position or size does not matter under the condition that suitable venting was sustained. Therefore, vacuum cooling offers an advantage for reducing storage costs, allowing a more tight package of products (Greidanus, 1971).

Additionally, vacuum cooling ensures hygienic expectations. Because only air goes into the chamber. When the seal is uncovered, the vacuum is released. Vacuum cooling also offers more precise temperature control by moderating the pressure (Longmore, 1973).

CHAPTER 2
DESIGN STUDY

In this part of the study, the vacuum compartment's system design for the household refrigerators will be explained. The essential components to be used in this design and the selection criteria will be answered. Additionally, the parameters that are decided as critical in system design and the details of these parameters will be included.

2.1 System Design

This study aims to adapt the vacuum system to household refrigerators. Compared to the vacuum cooling systems, this study's vacuum chamber does not have its cooling system. Instead, the cooling system of the refrigerator is used. The system designed for this study is shown in Figure 2.1.

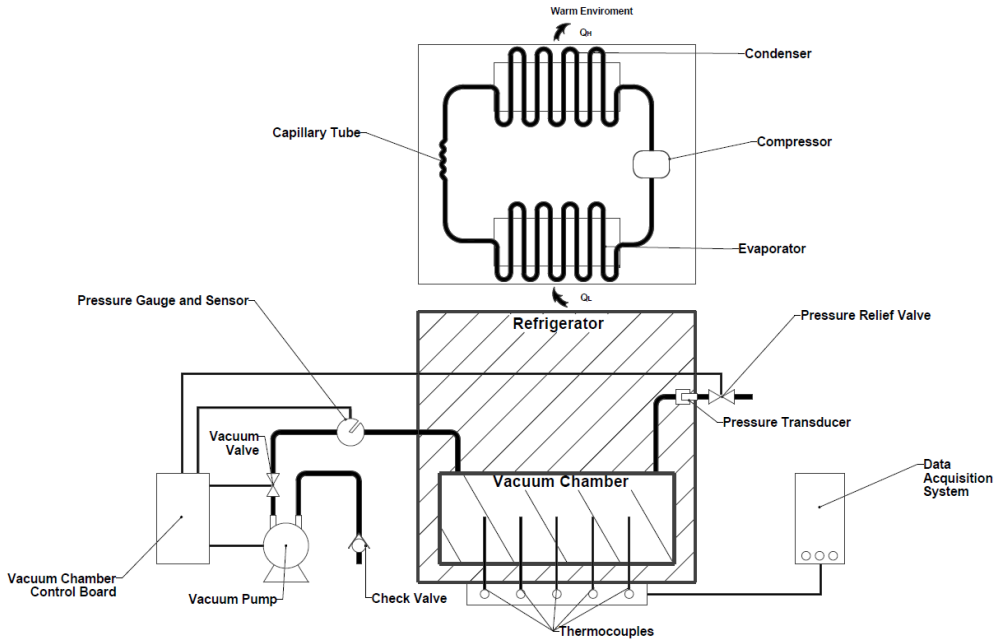

Figure 2.1-Schematic diagram of the vacuum system

As shown in Figure 2.1 there is a vacuum pump connected to the vacuum chamber and a pressure relief valve that balances the chamber pressure by taking air into the chamber when desired. The check valve, positioned at the vacuum pump's outlet end, allows a one-way air outlet from the vacuum pump. With a pressure sensor positioned between the vacuum pump and the chamber, the chamber's instantaneous pressure

value data is sent to the control card. The system works with an algorithm programmed into the control card. The control card controls the vacuum pump according to the data from the pressure sensor. Thermocouples placed in the vacuum chamber are placed for this study, and the temperature data in this vacuum chamber is sent to the data logger.

The vacuum chamber mentioned in this study was developed for household refrigerators for more extended storage of delicatessen products such as processed meats and dairies. Thus, the vacuum compartment was decided to be located at the coldest place of the cooler, the chiller zone.

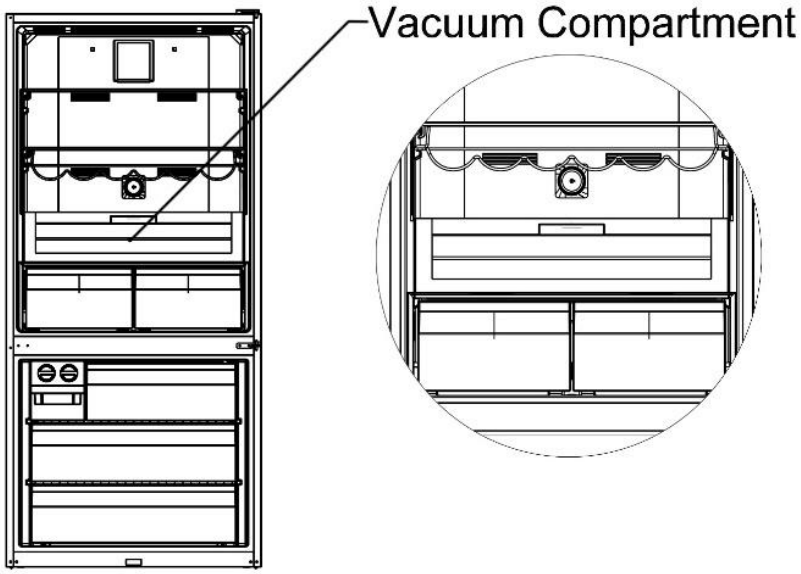

Figure 2.2 Location of the vacuum compartment

The system was designed, as shown in Figure 2.2, was located in a refrigerator that has a bottom freezer. As shown in Figure 2.2, the vacuum compartment was designed to replace the chiller zone.

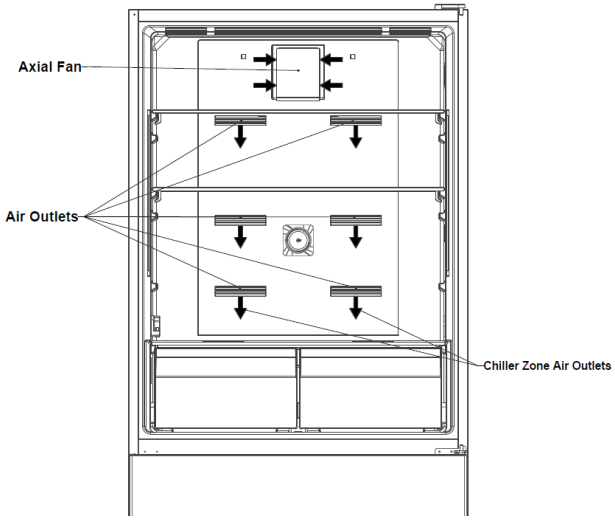

Figure 2.3 Airflow in the refrigerator

As shown in Figure 2.3, there is an axial fan at the top of the refrigerator. This fan draws the air in the refrigerator, drives it through an air duct with direct contact with the evaporator, and presses it from the air outlets. In the area where the vacuum chamber will be placed, there are air outlets of the chiller zone, and the coldest air in the cooler is in these air outlets.

The main components used in the vacuum system were vacuum chamber, vacuum drawer vacuum pump, hydraulic components, and air channels, as shown in Figure 2.4.

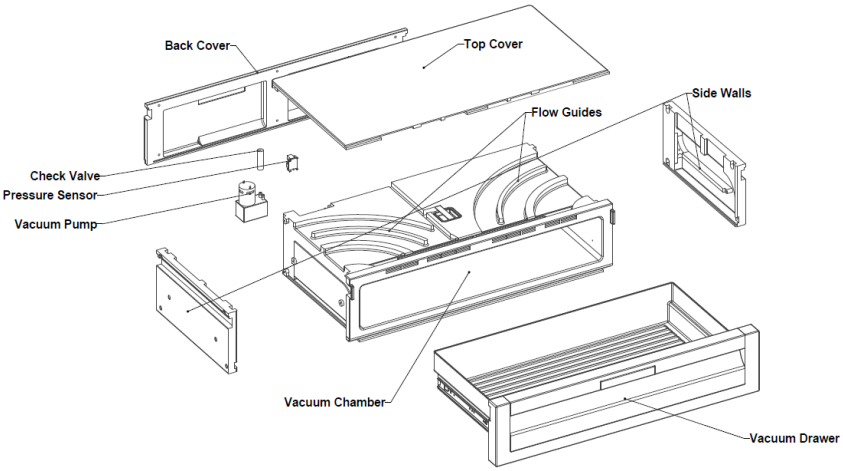

Figure 2.4 Components of the Vacuum System

In this study, the minimum vacuum value decided for the operation of the system is 0.5 bar. For this reason, 0.5 and 1 bar intervals have been considered when selecting the pressure sensor and vacuum pump. In addition to the targeted vacuum value, how often the pump will operate and how long it will discharge the air in the chamber is important for the selection criteria.

There are different types of Vacuum pumps. For the 0.5-1 bar vacuum range called a low vacuum, Positive displacement pumps are suitable for air applications. There are two types of positive displacement pumps in the market. They are Diaphragm pumps and rotary pumps. For this study, pump size is also essential. Therefore, a diaphragm type vacuum pump is suitable for the study.

Except for type, we need to choose the appropriate pump speed in the desired vacuum time range. As mentioned in the Vacuum cooling section of the Introduction chapter, the formula for finding a pump's pumping speed to reduce the vacuum chamber with a known volume to the desired pressure value in a certain period is as follows.

$$S = \eta \frac{V_f}{t}_{fp} ln \frac{P_{atm}}{P_{fp}} \tag{2.1}$$

If we neglect pump efficiency and simplify this equation for this study. The equation will be;

$$S = \frac{V}{t} ln \frac{P_{atm}}{P_1} \tag{2.2}$$

In the equation, S is the volumetric flow rate, and V is the volume of the vacuum chamber, t is the time, and P_1 is the desired end pressure of the vacuum chamber.

In this study, the Vacuum chamber volume is 26 l, and the vacuum pump is working in 1 bar - 0.5 bar and 0.7 bar - 0.5 bar intervals. As we consider the user comfort, a long vacuum pump operating time is not desired in a household-type refrigerator. The maximum evacuation time in this study was considered to be 5 minutes. Therefore, with the equation, the flow rate must be 3.91 lt/min.

Boxer 3KD series diaphragm pump is selected for the vacuum system. As shown in Figure 2.5, the free flow of the pump is 18 l/min. However, the flow rate is changing with pressure.

Figure 2.5 Boxer 3KD diaphragm pump technical data (Boxer Pumps, 2021)

When the pump's flow curve is examined in Figure 2.6, the average flow rate for the 1-0.5 bar range is calculated as 8.48 l / min. This flow rate will be 4.73 l / min for the range of 0.7-0.5 bar.

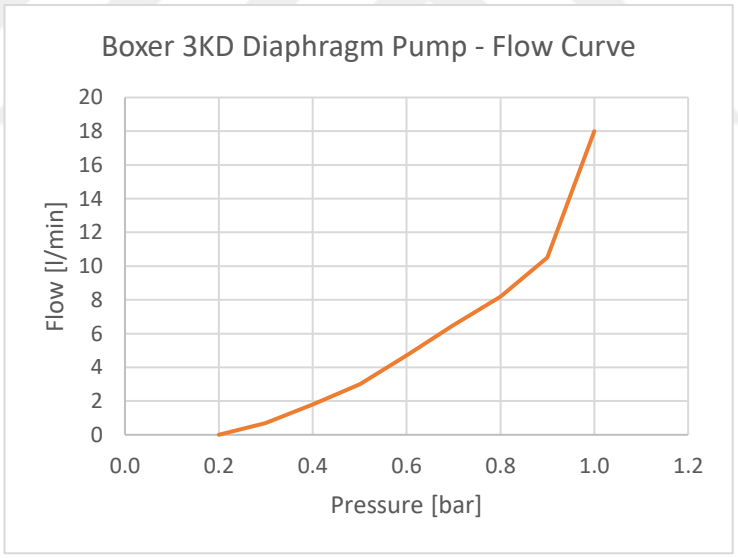

Figure 2.6 Flow curve of Boxer 3KD diaphragm pump (Boxer Pumps, 2021)

2.2 Parametric Study

As mentioned before, the vacuum compartment was decided to be located at the cooler's coldest place, the chiller zone. Therefore, the compartment had a dimension limitation.

As shown in Figure 2.7, the air enters from the rear part of the vacuum chamber, passes under the chamber, and then exits from the front part by going around the sidewalls and the top of the chamber, respectively.

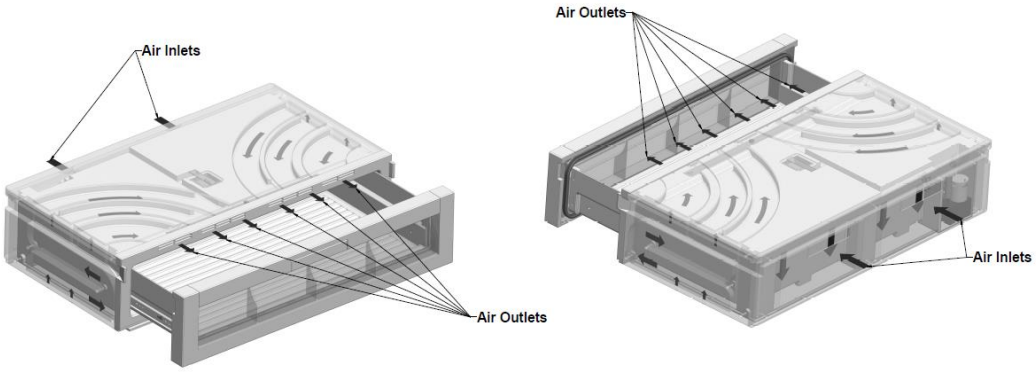

Figure 2.7 Air paths in the vacuum system

Expanding the vacuum chamber volume was one of the main aims of this study. As shown in Figure 2.8, compartment height and width were constant, and air channels were placed in these dimensions. These channels reduced the usage area of the vacuum chamber. To maximize the volume, the air channels of the vacuum compartment must be as small as possible.

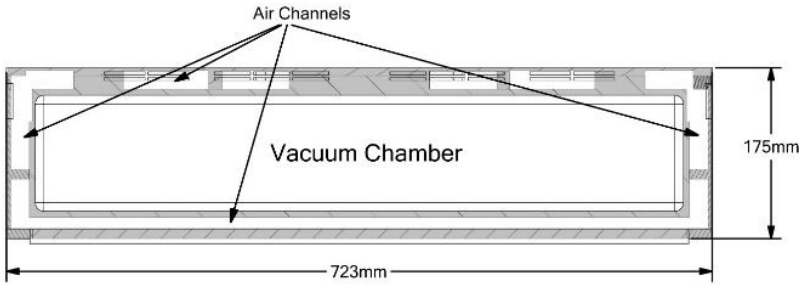

Figure 2.8 Dimension limitations and air channels

On the other hand, the temperature distribution of the vacuum chamber was another critical parameter.

In this study, flow guides were placed into the air channels for enhancing the homogeneity of the temperature distribution at the vacuum chamber. These guides were shown in Figure 2.9.

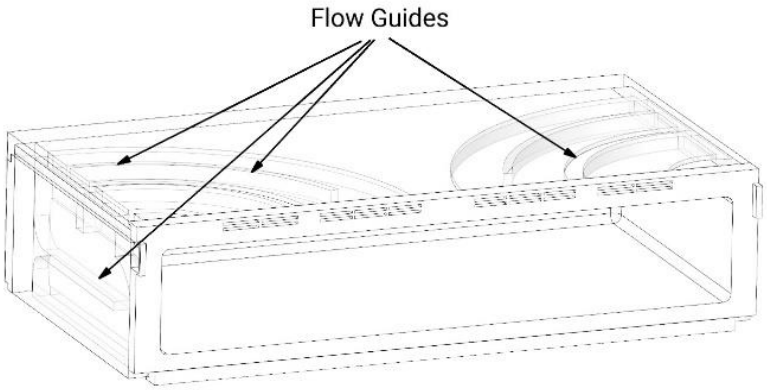

Figure 2.9 Flow guides of the vacuum compartments

The channel width and the flow guides both affected the pressure drop of the channel. Therefore, the velocity inside the air channel also a vital parameter for balancing the pressure drop. It is also critical for the vacuum chamber's cooling time, which is one of the main goals for this study.

Based on all these facts, channel width and flow guides were selected as geometric parameters, and air velocity was selected as an input parameter for the numerical study. The numerical study's output parameters were the vacuum chamber's average temperature, average outlet temperature, and pressure drop.

CHAPTER 3
NUMERICAL STUDY

Computational fluid dynamics (CFD) methods are used in the numerical study. Ansys 2019 R1 computer-aided engineering (CAE) software is used in the study, and it includes different steps for the CFD study.

This section details how geometry is prepared, domains are selected, meshing details, boundary and domain conditions, and calculations methods.

3.1 Domain Geometry

The geometry used in this study, based on the geometric limits of the refrigerator chiller, is designed using Creo Parametric V4.0 (PTC Inc., Boston, MA, USA) Computer-Aided Design (CAD) software.

The model was simplified by eliminating small edges, joining faces, and defeaturing the details created for the structural design, which will not affect the flow for preparing the geometry that provides enhanced meshing. The system was designed according to its symmetry axis. Thus, the half model was used to reduce the number of elements and shorten the solution time.

The simplified model for the numerical solution designed with the engineering approach is shown in Figure 3.1.

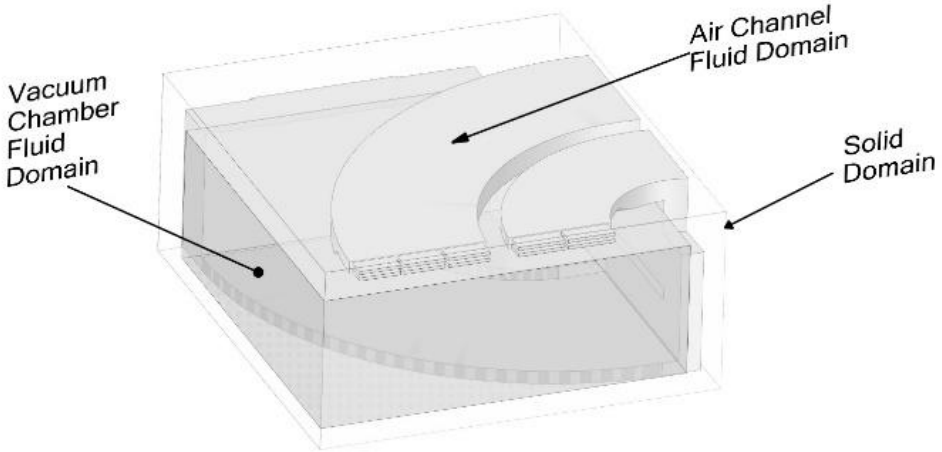

Figure 3.1 The simplified model for the numerical study

Figure 3.1 shows the three domains defined for the numerical study as vacuum fluid domain for the vacuum chamber, air channel fluid domain for air ducts which encloses the vacuum chamber, and polystyrene solid domain for the main body.

3.2 Meshing

For the design and optimization studies, computational time is one of the critical factors determining a CFD solution's effectiveness. Finer meshes increase the computational time and dramatically increases the computational cost. It is necessary to divide the domains into the finite elements in which the numerical analysis was performed. The 3D model created in this study was divided into finite elements using ANSYS Meshing V19.3.

The mesh and mesh details were used in this study, as shown in Figure 3.2. Sweep method used in the vacuum chamber and the air channel fluid domain to reduce the number of elements. Mesh refinements like curvature adaptation for curves and proximity for narrow areas are available for a more reliable mesh.

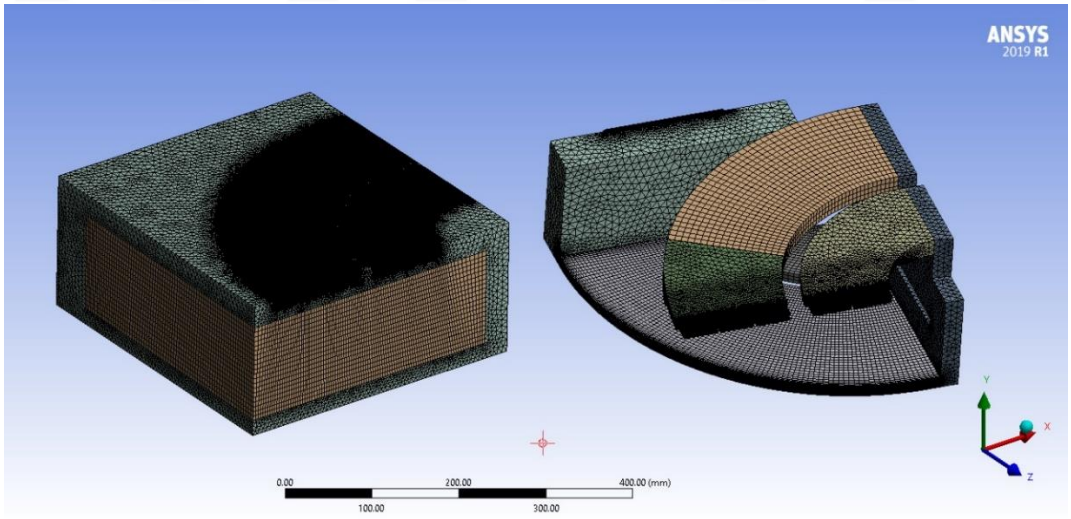

Figure 3.2 Meshes of the domains

An inflation layer meshing strategy was added for refining the air channel mesh, as shown in *Figure 3.3*. According to Mara et al., near-wall region flow behaviour is complex and needs to be captured appropriately to trust the CFD results (Mara et al.,

2014). The velocity decreases in a nonlinear manner when coming closer to the wall of an object. The inflation layer strategy was used to capturing the rapid changes of the near the wall flow. This method allows the boundary layer for turbulent flow to be captured and evaluated in high resolution.

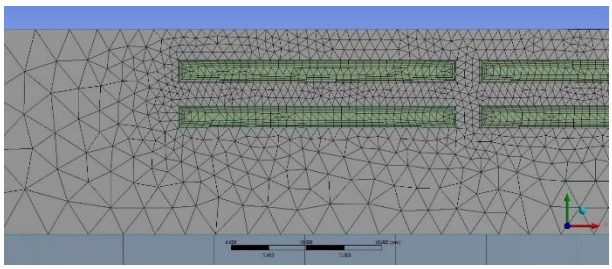

Figure 3.3 Inflation layer detail

3.2.1 Mesh Independency

All parameters in a CFD solution, i.e. mesh size, convergence criteria, time step size, define a convenient CFD solution's success. Increasing the number of elements is generally improves the precision of CFD solutions (Sørensen , 2003; Tu et al., 2018). Increasing the element quantity in computational geometry is performed until a mesh independent solution is achieved. This is a general rule (Sørensen, 2003; Wang & Zhai, 2012). In the end, this should ensure a minimum difference between the solutions. However, this increases the computational time (Norton & Sun, 2006). Due to computational power limitations, the large quantities of mesh elements may not always be obtainable. Using coarser meshes can still give precise results opposite to the theory of fine mesh resolution for high accuracy.

As shown in Table 3.1, 4 numerical models with different mesh sizes were created in this study. Besides, the results of the average outlet temperature were investigated for 4 cases. As shown in Figure 3.4, the temperature difference between case 4 and case 3 is 0.01 °C. Thus, Case 3, which has 5447141 elements, was used to reduce the number of elements and shorten the solution's time.

Table 3.1 Effect of the mesh size to the average outlet temperature

	Number of Elements	**Average Outlet Temperature [C]**
Case 1	1280296	-10.56
Case 2	3124398	-10.55
Case 3	5447141	-12.07
Case 4	11157496	-12.06

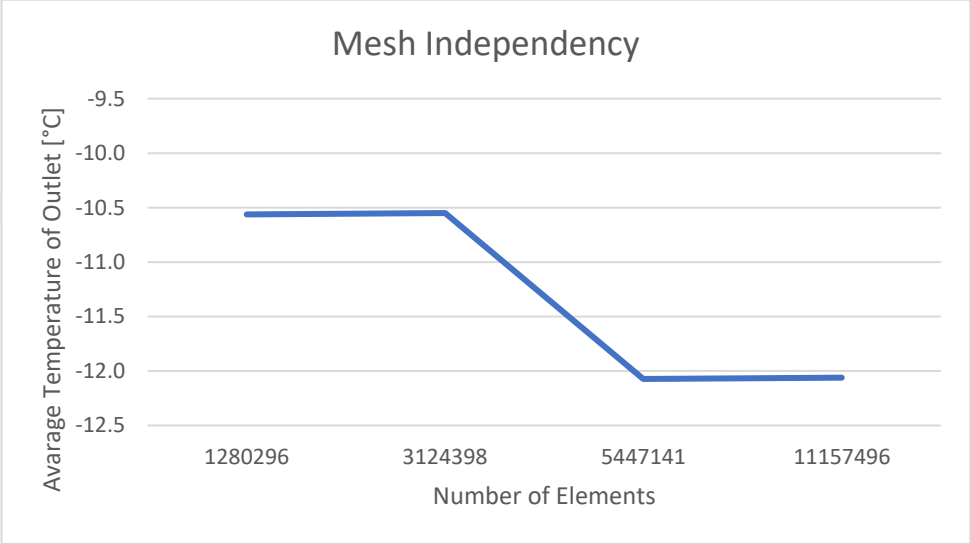

Figure 3.4 Mesh independency

3.3 Physics and Boundary Conditions

The half-modelled flow domain's boundary conditions considering the model's symmetry plane are given in Table 3.2. The input was defined as a velocity inlet with constant velocity, and the output was defined as a pressure outlet with 0 relative pressure.

Table 3.2 Boundary conditions

Domain	**Boundary Condition**
Vacuum chamber domain	Symmetry
	Wall with 4 °c static temperature
	Fluid-solid interface
Air channel domain	Inlet with 2 m/s constant speed and -6°C static temperature
	Outlet with average static pressure with 0 Pa relative pressure
Solid domain	Symmetry
	Adiabatic wall
	Wall with 4 °c static temperature

The inlet velocity value is determined as a design parameter and defined as 2 m/s for the first study. This average velocity and the inlet temperature are measured by the Omega TVS-1100 Series Velocity and Temperature Measuring System from the refrigerator's actual air duct outlet, as shown in Figure 3.5.

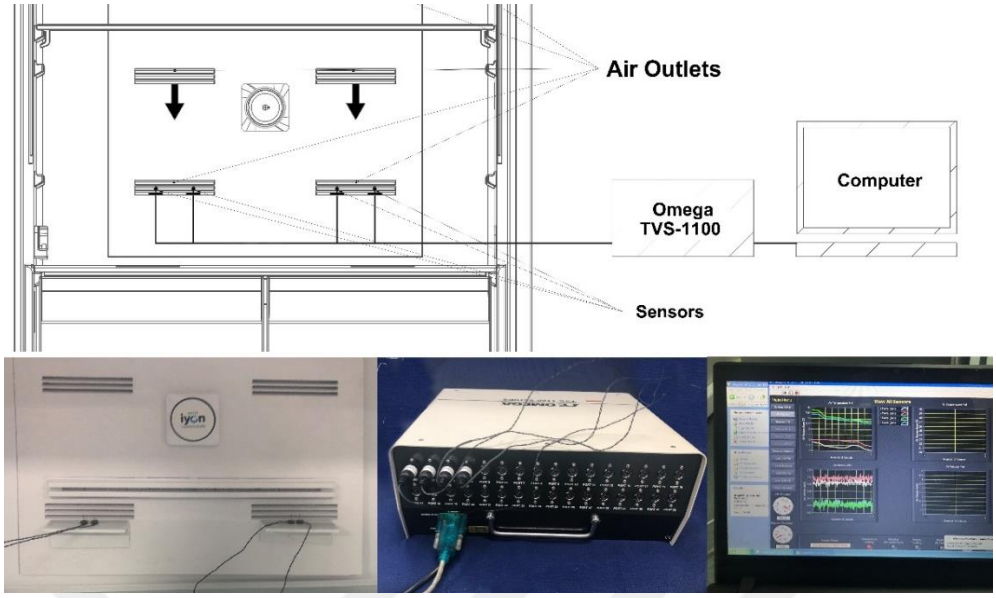

Figure 3.5 Inlet velocity test setup (Personal archive, 2020)

3.4 Solver

The CFD calculations were performed with a transient analysis type for a total time of 150 seconds with a time-step size of 10s. Later in the thesis, the topic of time independence was also addressed. The flow behaviour was simulated using a standard k-ε turbulence model with scalable wall function. The total energy heat transfer model and Monte Carlo thermal radiation model were used for energy and heat transfer behaviour. The Finite Volume Approach was applied, and the method is resulted with discretized governing equations. The high-resolution scheme was preferred since it is more robust. A second-order backward Euler Transient Scheme was applied.

3.4.1 Time Independency

Acquiring accurate results at the lowest CPU cost is always an import goal of a CFD study. The time step length and number of iterations in the one time-step are significant factors that affect the numerical accuracy and convergence time. Long-time steps can save solution time for transient cases. However, it can cost numerical accuracy. For complex geometries or studies with high Reynolds numbers, large time steps can even diverge the computation.

Sensitivity studies were carried out to obtain results that were independent of the time step. For achieving that, three different time step sizes of 1s, 5s and 10s have been chosen. The number of elements was set to 5447141 for all studies. The average outlet temperature recorded with respect to the variation of time step size were given in Figure 3.6. The temperature for a time-step size of 1s, 5s, and 10s does not change magnificently. Nevertheless, minor variations in the calculation results involve a lot of computation time even in the case of decreasing the time step size under 10 seconds. Therefore, the optimum time step size is determined as 10s in this case.

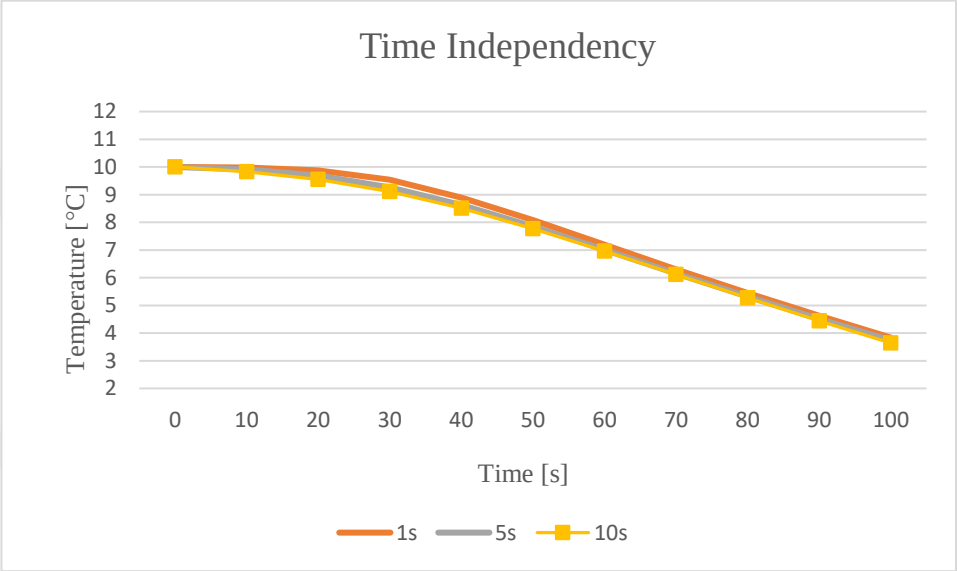

Figure 3.6 Time independency

CHAPTER 4
RESULTS OF THE NUMERICAL STUDY

The CFD results of the design points are given in Table 4.1 and Figure 4.1. As Table 4.1 investigated, flow guides increase the pressure drop. The same effect also occurs when the channel width decreases. However, as the channel width decreases, the vacuum chamber volume can be expanded by 8.49%.

Table 4.1 Results of Design Points

Design Point	**unit**	**DP 1**	**DP 2**	**DP 3**	**DP 4**	**DP 5**	**DP 6**	**DP 7**	**DP 8**
Channel Width	**[mm]**	12	12	12	12	20	20	20	20
Speed	**[m/s ^2]**	2	1	2	1	2	1	2	1
Flow Guides	**Yes/ No**	Yes	Yes	No	No	Yes	Yes	No	No
Average temp of the chamber at 150 s	**[°C]**	0.65	1.85	-0.59	1.14	0.25	2.25	0.09	1.8
Time of vacuum chamber at 0°C	**[s]**	164	200	139	172	155	195	152	187
Outlet Average Temp at 150sn	**[°C]**	-11.95	-11.35	-11.36	-10.51	-9.75	-7.95	-11.26	-10.38
Pressure Difference outlet-inlet	**[Pa]**	-455.9	-112.7	-37	-9.39	-181.5	-44.78	-34.03	-8.68
Chamber Volume	**[l]**	28.27	28.27	28.27	28.27	26.09	26.09	26.09	26.09

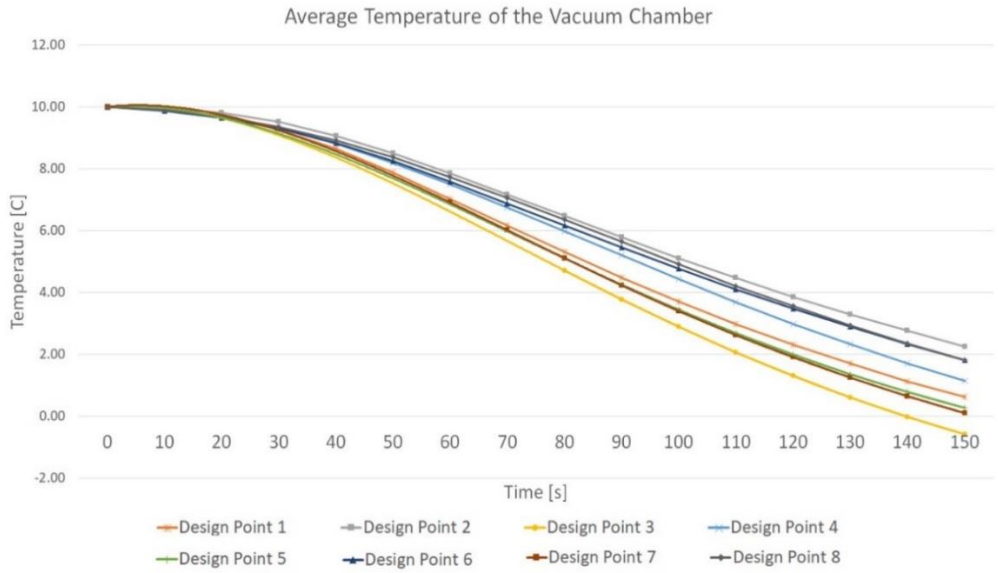

Figure 4.1 The average temperature of the vacuum chamber through time

If we increase the flow velocity 1 m/s to 2 m/s, it decreases the cooling time 10 °C to 0 °C an average of 36s which means 19.1% faster cooling. On the other hand, it increases the pressure drop significantly. 2 m/s analysis averagely has 4.03 times more pressure drop than 1 m/s.

With all these effects evaluated together, Design Point 3 seems the most beneficial design. It has the minimum average temperature in the vacuum chamber at t=150 and has one of the lowest pressure drops.

Nevertheless, another important phenomenon is the thermal uniformity of the vacuum chamber. Figure 4.2 shows the temperature distribution and velocity streamlines in the vacuum chamber in the presence or absence of flow guides.

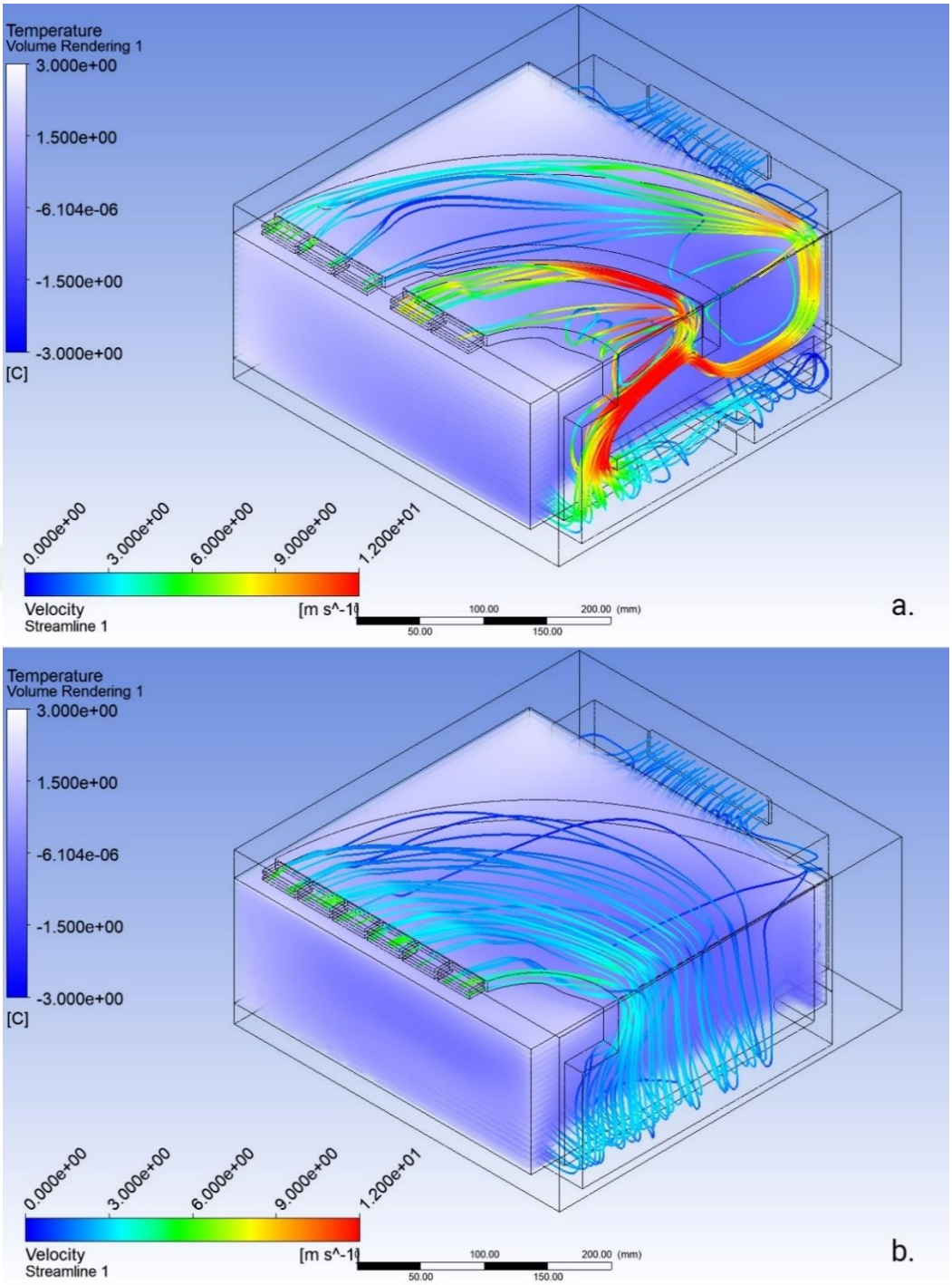

Figure 4.2 Temperature distribution at vacuum chamber and velocity streamline a. with flow guides b. without the flow guides

The normalized temperature histogram of the vacuum volume was given in Figure 4.3 for investigating this.

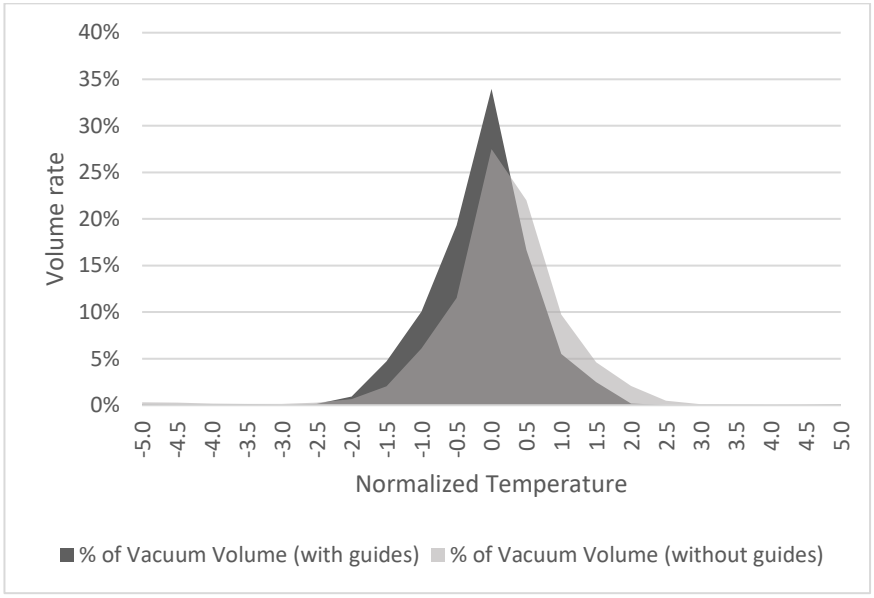

Figure 4.3 Normalized temperature histogram of vacuum volume with and without the flow guides

In Figure 4.3, temperature values are normalized by the histogram's peak value for a more straightforward comparison of the temperature distribution. 0 Point at the X-axis represents the peak position of the histogram. Positive and negative values correspond to the point, which has a higher or lower temperature than the median temperature. As Figure 4.3 examined, the histogram of the model with flow guides has a higher peak point and a smaller base. Therefore, it can be said that the model with the flow guides has better thermal uniformity than the model without flow guides.

As Figure 4.3 and Table 4.1 evaluated together, flow guides increase thermal uniformity and the pressure drop. Because of the pressure drop, they must be considered a new design parameter for further studies.

The numerical study aimed to investigate the aerodynamic design of the vacuum chamber cooling channels and evaluate affecting parameters. Channel parameters were simulated by using transient CFD analysis. In these analyses, both air inside the cooling channel and the vacuum chamber's air was modelled. The radiation was also

considered besides the natural convection. Mesh independency and time-independent studies, which are essential for the correctness of the analysis also carried out.

Regarding the results based on the air channel width parameter, 12 mm channel width has better performance due to its larger vacuum volume and shorter cooling time, but it increases the system's pressure drop. In this case, it may be considered to increase the system's fan power to prevent this pressure loss from disturbing the system balance.

The analysis shows that flow guides succeed the purpose of enhancing the temperature distribution inside the vacuum chamber. However, they dramatically increase the pressure drop, so they must be developed in the aerodynamic sense in further design studies.

CHAPTER 5
EXPERIMENTAL STUDY

5.1 Proof of Concept (POC) Prototype

The design parameters of the vacuum chamber to be built were determined in the previous section. Among these parameters, three parameters that are critical for us are as follows.

- Channel width: 12 mm
- The axial fan speed of the refrigerator: High-speed axial fan with 2 m/s chiller zone outlet speed.
- Flow guides

As mentioned in the previous sections, the cold air coming from the refrigerator air duct will be filled around the compartment. The design of these ducts aims to send the incoming air around the whole compartment and send it into the refrigerator. As seen in the numerical study, flow guides are crucial for the thermal distribution in the vacuum chamber, and while designing the test prototype, the flow is aimed to circulate the whole chamber.

While designing the POC prototype, besides the above parameters, the design was made by considering the manufacturability, ergonomics, and sealing parameters.

The main components to be used in the prototype are the vacuum pump, pressure sensor, check valve, control card, and vacuum chamber. There are a pressure sensor and a check valve between the pump and the vacuum chamber. The sensor monitors the vacuum value of the compartment instantly and transmits this data to the control card. As the check valve allows one-way flow from the line on the pump after vacuuming, it prevents the chamber from taking air from the pump line.

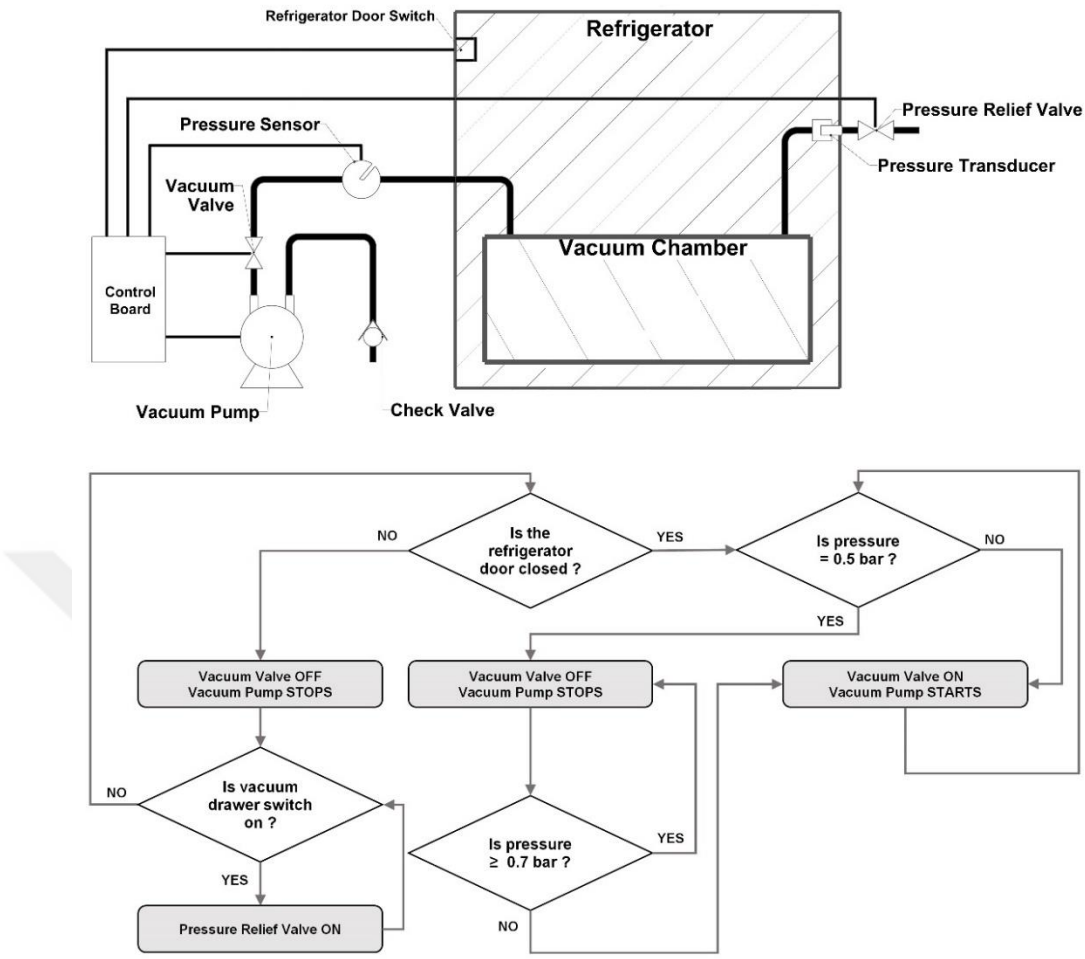

Figure 5.1 Algorithm of the system

As seen in Figure 5.1, the working algorithm of the system is as follows.

When the refrigerator door is closed, the vacuum pump will start working with the control card's signal. The pressure sensor controls the vacuum chamber pressure, and the pump will continue to operate until the desired pressure level is reached to 0.5 bar. When the pressure value is 0.5 bar, the pump will stop working.

Sealing is a crucial factor in vacuum chamber design. Although this system is designed to be impermeable, the compartment will have air leakage. In this case, the desired vacuum value will decrease over time until the pressure sensor reads 0.7 bar. After that, the pump will re-engage and until the pressure back to the 0.5 bar

User comfort and ergonomics are important points when designing the POC prototype. For this reason, the vacuum compartment is designed as a railed drawer. The rails are fixed in a drawer attached to the compartment cover and have a sealing gasket. In this design, the spring mechanism in the selected rails is activated at the last point of the drawer's closure and fully presses the lid and its gasket to the vacuum chamber.

When the user wants to open the vacuum drawer, the chamber will not open due to the chamber's negative pressure. For this situation, a pressure relief valve has been added to the system, which will be activated and allows air into the compartment when the user tries to open the drawer to open the compartment easily.

Figure 5.2 POC Prototype images (Personal archive, 2020)

As shown in Figure 5.2, the prototype was produced according to the design criteria outlined in this section and placed in the Vestel NFK640-EX refrigerator. POC Prototype will be tested in the next section. Then, it will be finalized after the optimization and improvement studies.

5.2 Measurement Of Thermal Behaviour.

As exhibited in Figure 5.3, the vacuum system's temperatures were measured by connecting 6 OMEGA T type thermocouples in the test set up for the Vacuum system's temperature test. The accuracy of the thermocouples is ± 1°C, as mentioned in the manufacturer's datasheet. The measurements taken were collected with the HIOKI LR8400-20 data logger and transferred to the computer for evaluation (Omega, 2021).

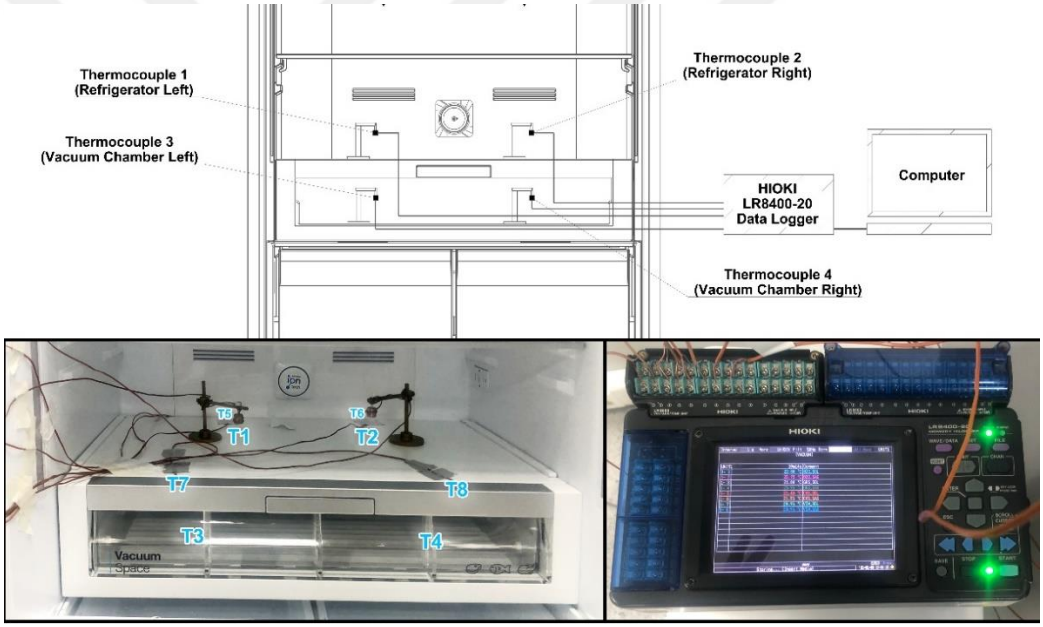

Figure 5.3 Experiment setup for measuring the thermal behaviour (Personal archive, 2020)

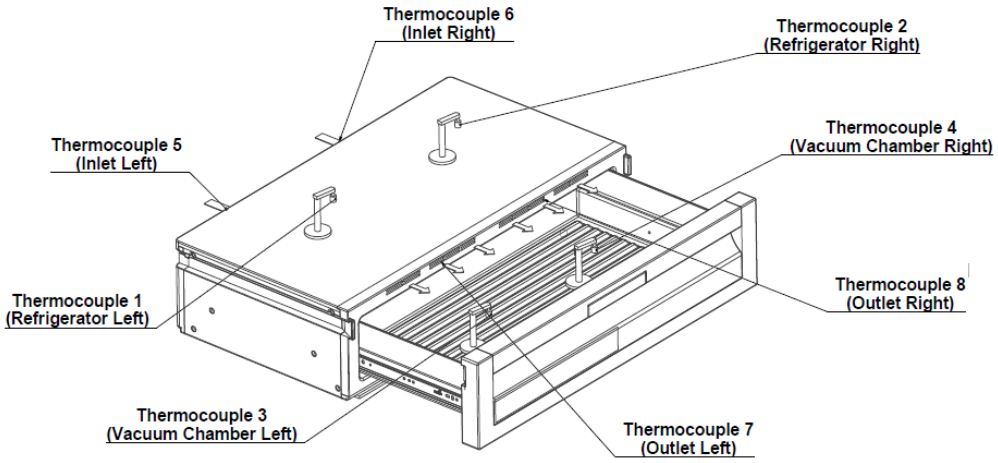

Figure 5.4 Thermocouple positions

As shown in Figure 5.4, T1 and T2 thermocouples are placed above the compartment to measure refrigerator temperatures. T3 and T4 thermocouples are placed in the vacuum compartment to measure the temperature of the vacuum compartment. Additional two thermocouples (T5 and T6) are positioned in the air channel inlets to measure the vacuum system's inlet temperatures. T7 and T8 thermocouples are placed at the air channel outlets to measure the vacuum system's outlet temperatures.

Besides measuring refrigerator temperatures, the operating ranges and the pump's power consumption connected to the vacuum chamber were also monitored with the data logger. In this way, it was observed how often the compartment reached a low-pressure value and how much an effect it had on the refrigerator's energy level and the refrigerator's operation.

5.3 Observation of Food Shelf Life Behaviour

The effect of the vacuum system on foods is one of the key aims of this study. For observing the vacuum chamber's effect on food shelf life, 12 delicatessen product samples with the same expiration date were placed in the vacuum chamber and

refrigerator compartment in closed containers. Chosen delicatessen products are the foods that users usually put in the chiller compartment. The list of the products is given in Table 5.1.

Table 5.1 Sample food list

	Chicken Ham	**Salami**	**Sausage**	**Bologna**	**Feta Cheese**	**Cheddar Cheese**
Vacuum Chamber	Sample 1	Sample 2	Sample 3	Sample 4	Sample 5	Sample 6
Refrigerator	Sample 7	Sample 9	Sample 10	Sample 8	Sample 11	Sample 12

Sensory tests (eye control, odour control) were carried out between foods in 2 different compartments at the start at 76 hours and 92 hours after the start of the test. During these controls, the product photos were taken under constant light simultaneously, and the results were documented.

CHAPTER 6
DESIGN VALIDATION AND RESULTS OF THE EXPERIMENTAL STUDY

In this section, the thermal test results and the food observation results of the vacuum system design will be explained to validate the system. Furthermore, the last part will include the comparison of the experimental results with the numerical study, which can be used for design optimization processes.

6.1 Thermal Design Validation

In this section, the thermal results of the vacuum chamber for household refrigerators will be explained.

After the thermocouples were placed at the vacuum compartment's critical points in the refrigerator and refrigerator, the refrigerator cooler compartment was adjusted to 4 degrees, and the refrigerator started to operate. When the refrigerator door is closed, the vacuum system was activated and reduced the vacuum compartment's pressure to a 0.5 bar.

After the test setup was set up, this test continued for 35 hours. During this test, while the refrigerator temperatures were monitored, the vacuum system's energy consumption also recorded.

The measurement results obtained from the thermocouples placed in different parts of the test setup as the right and left sides of each zone are shown in Figure 6.1.

When the temperatures taken from different points of the vacuum chamber shown in Figure 6.1 are examined, the maximum temperature difference was measured as 0.45 ° C. Therefore, the average temperatures of the regions at the measurement points are calculated for evaluating the system.

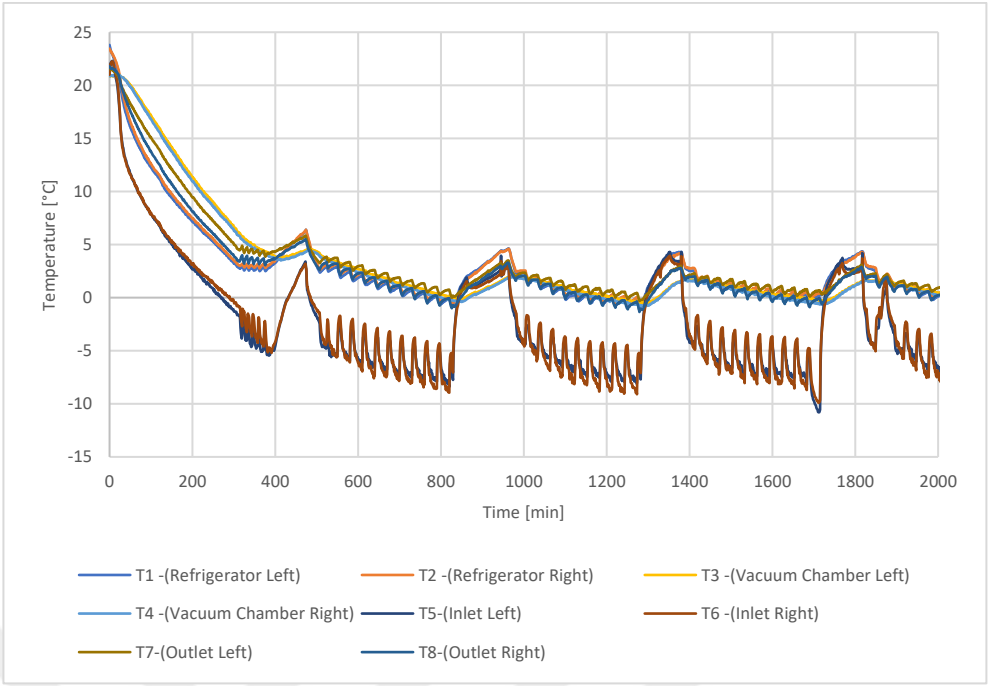

Figure 6.1 Thermal measurements of the POC prototype at measurement points

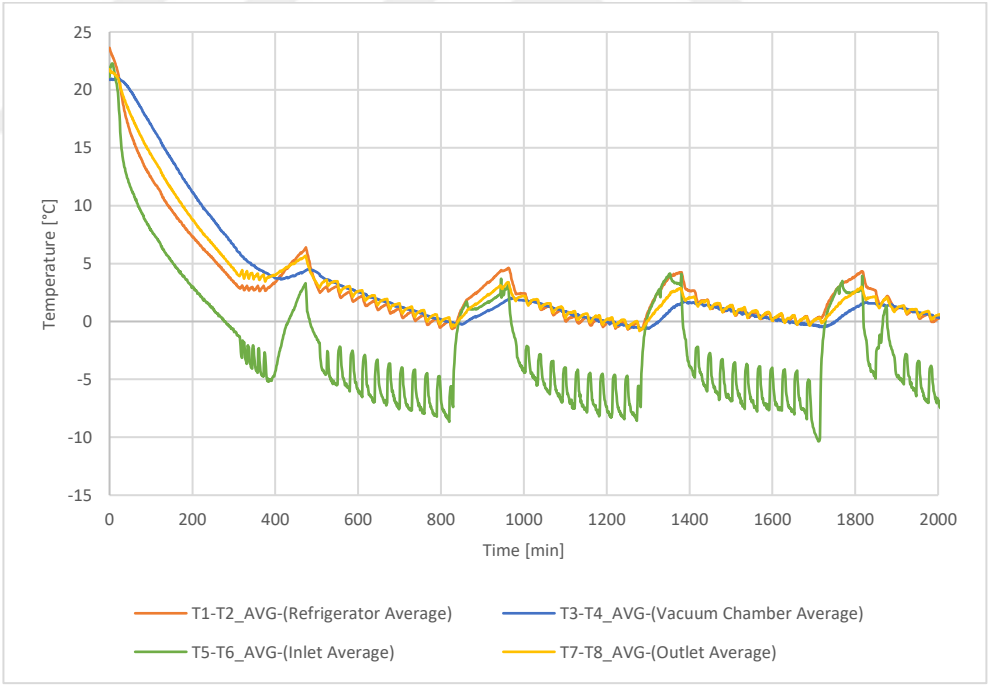

Figure 6.2 Calculated averages of thermal measurements of the POC prototype

Figure 6.2 shows the calculated average temperatures of the compartments. When Figure 6.2 is examined, the refrigerator's initial internal temperature is room

temperature. After around eight hours, its cycle stabilized. The air at the inlet of the vacuum chamber air ducts is at an average of -5 °C.

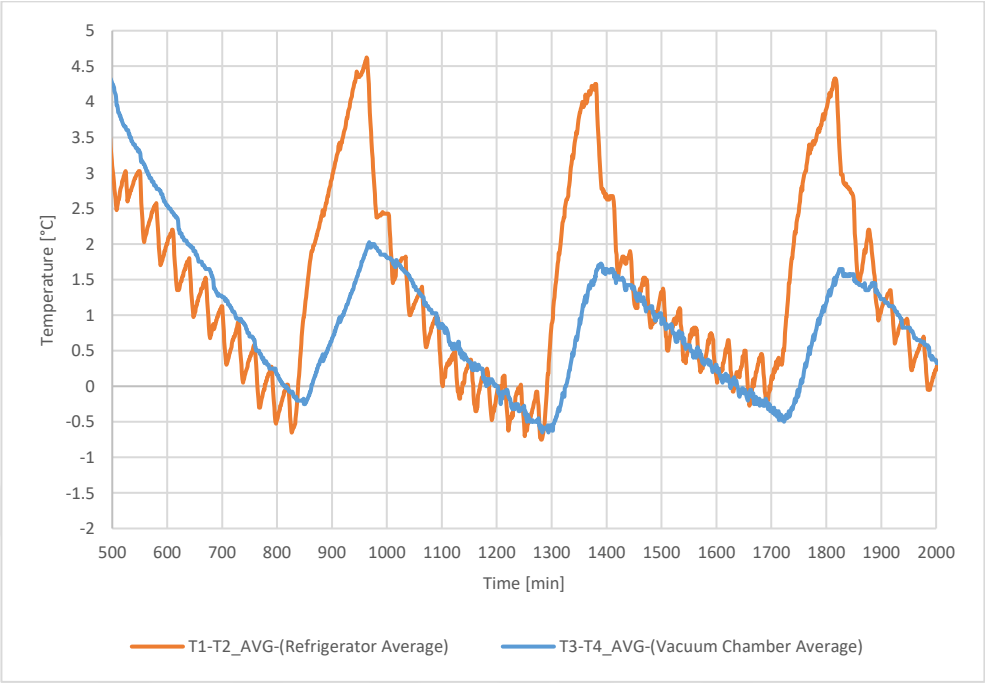

Figure 6.3 Calculated averages of thermal measurements of the vacuum chamber and the refrigerator cooler after 8 hours

Figure 6.3 shows the temperature comparison graph of the vacuum compartment and the refrigerator cooler compartment when the refrigerator is balanced at the end of 8 hours. As seen in the graph, the refrigerator's temperature in the cooler compartment varied with an oscillation between 5 °C and 0 °C, while the temperature in the vacuum compartment showed an oscillation between 2 °C and 0 °C. This result shows that the vacuum chamber is more resistant to thermal changes since the heat transfer mechanisms do not include convection. So, it cools and heats more slowly than the regular compartments of the refrigerator.

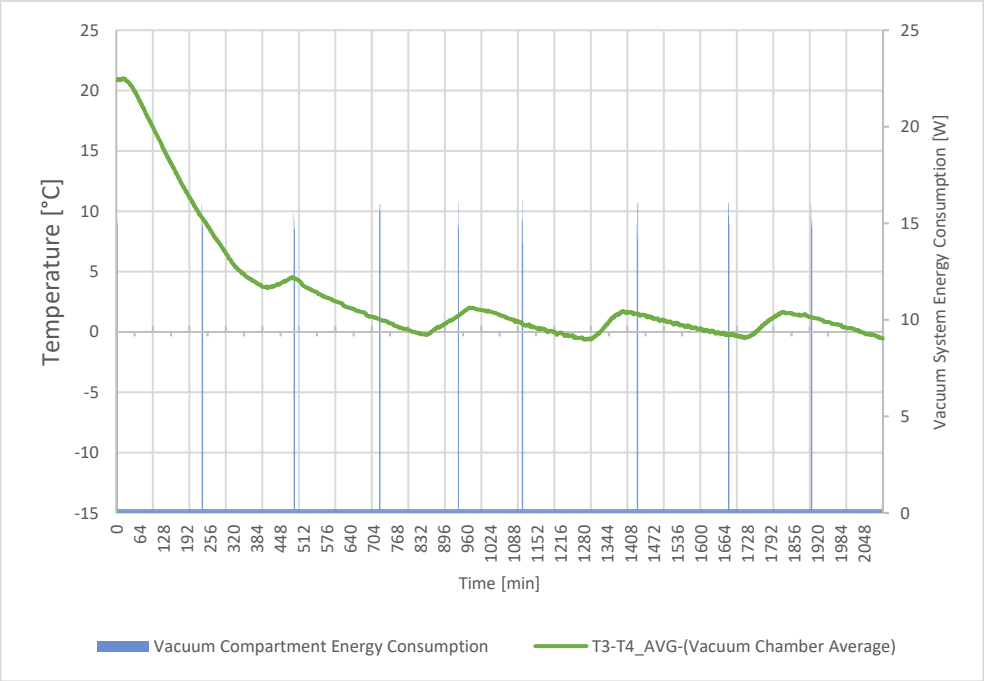

Figure 6.4 Calculated averages of thermal measurements of the vacuum chamber and energy consumption of the vacuum system

During this experimental study, while the refrigerator and vacuum compartment's temperatures were measured, the energy consumed by the vacuum compartment was also observed. Figure 6.4 shows the temperature variation of the vacuum chamber and the power graphs of the vacuum pump. As seen in the experimental study result, when the vacuum pump is activated, the pump consumes an average of 15 W of energy and stays on for an average of 3 minutes. The pump reduces the compartment pressure to 0.5 bar in every activation. Then, the pressure rises to 0.7 bar again, approximately 4 hours and the pump is reactivated with the sensor's data and the command sent by the control card. This cycle repeats itself every 4 hours on average. When the experimental results are examined, it is calculated that the vacuum system consumes 0.75 Wh energy in 4 hours in addition to the energy load of the refrigerator. According to this calculation, when the vacuum compartment energy consumption is analyzed annually, it is seen that the refrigerator will add 1.62 kWh to the annual energy consumption. Vestel NFK640 EX refrigerator energy consumption used in system design is 371 kWh/year. Therefore, the vacuum compartment increases the refrigerator's energy consumption by 0.43%. Furthermore, this increase is minor in energy consumption to reduce the refrigerator energy class.

6.2 Food Shelf Life Test Results

Delicatessen foods with the same expiration date at the beginning of the test, shown in Table 5.1, were divided into two separate groups: refrigerator cooler compartment products and vacuum compartment products.

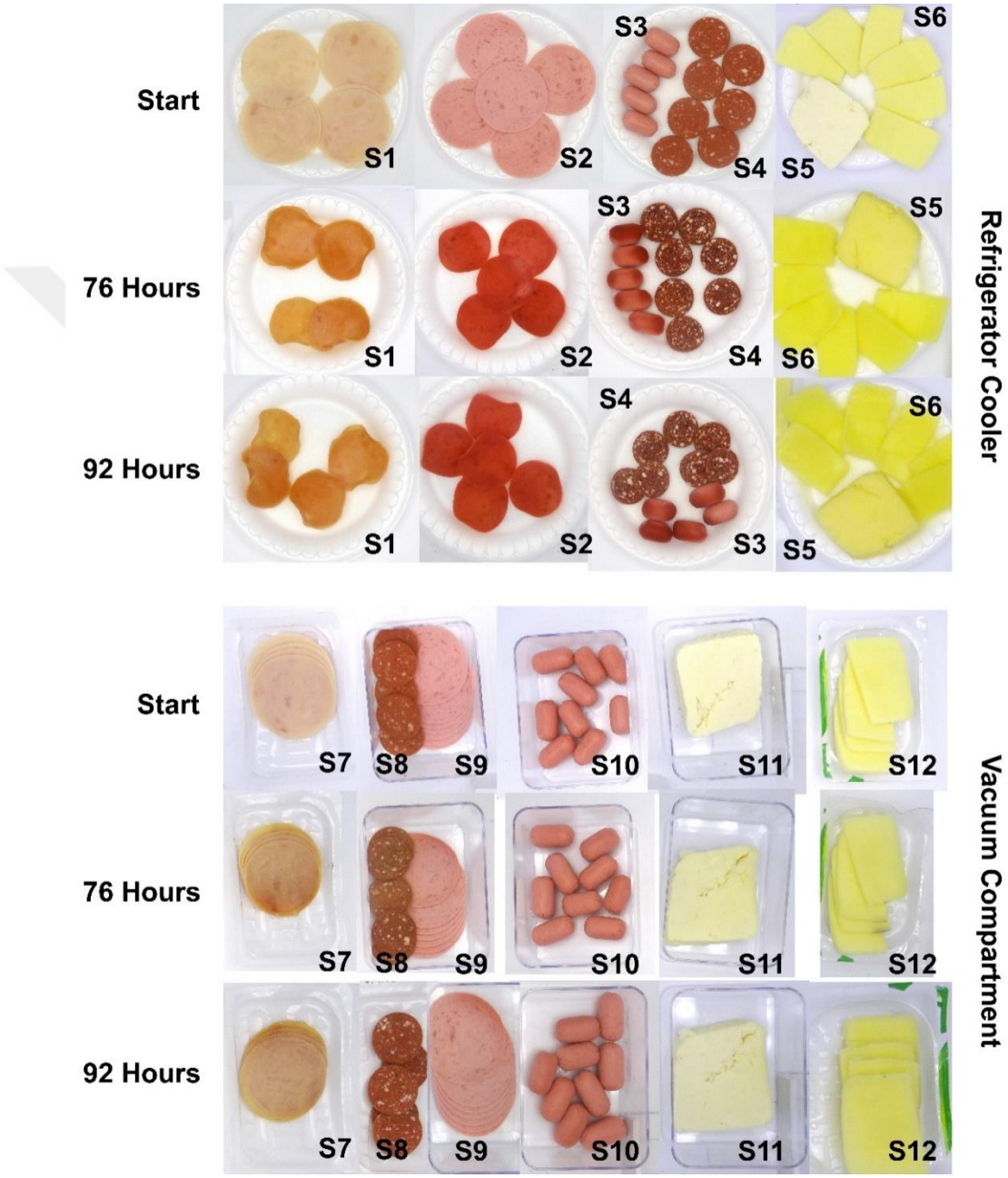

Figure 6.5 Food shelf life sample photos at different periods (Personal archive, 2020)

Visuals in the start rows of Figure 6.5 are the visuals of foods before they are placed in the refrigerator, and the images in the first line of the upper group are the products in the refrigerator compartment, and the images in the top row of the lower group are the first versions of the products in the vacuum compartment.

The products were placed in the steady working refrigerator's cooler and vacuum compartments. After 76 hours, the products were taken out of the refrigerator for examination. As shown in the 2nd rows of the visual groups in Figure 6.5, a large extent of drying and spoilage was observed in all products in the refrigerator cooler compartment. On the other hand, all products, except chicken ham, remain in their initial state from the vacuum chamber products. Partial drying has begun in chicken ham.

After the first examination of the products, the products were placed back in the refrigerator and vacuum compartment, and the test continued. When the total test time was 92 hours, the products were taken out again, and the second observation stage was carried out. As can be seen in the 3rd rows of the visual groups in Figure 6.5, in this 2nd observation, all products in the refrigerator cooler completely spoiled and partial spoilage and drying started in the products in the vacuum compartment.

6.3 Evaluation and The Validation of The Numerical Model

After completing the design validation, the CFD study was revisited for experimental validation purposes to investigate the numerical modelling method's success.

As mentioned in chapter 3, the refrigerator's cycles were not model since the numerical model does not consist of the refrigerator's full internal volume. Although modelling a full refrigerator with the vacuum chamber is on further study plans, it is not in this thesis's scope.

Therefore, the average temperature after initial cooling is calculated from the experimental data. The comparison between this data and the numerical study is given in Figure 6.6. As aforementioned, the pressure of the vacuum chamber changes

between 0.5 Bar and 0.7 Bar. Two analysis were performed to simulate these maximum and minimum pressure conditions.

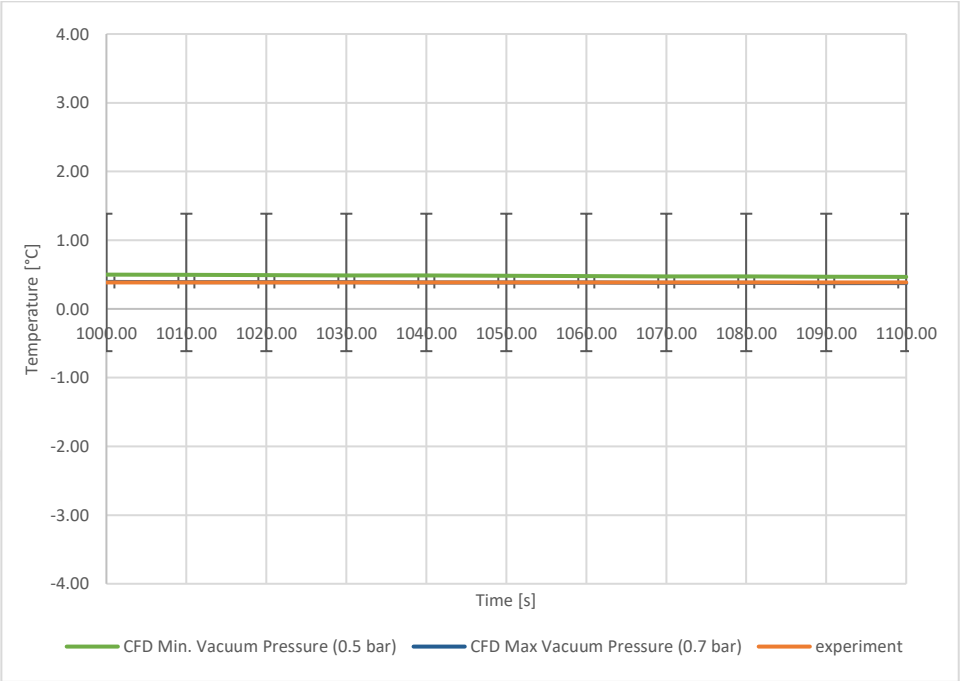

Figure 6.6 Comparison between CFD and experiment results

Figure 6.6 show that the CFD results are in good agreement with the average experimental result. The average absolute error between the 0.5 Bar CFD analysis and the experiment is 0.1 K, regarding a -0.04% error ratio on the Kelvin scale.

In the light of these results, it can be said that the numerical model and the physical assumptions are valid for a realistic simulation of the vacuum chamber, which can be used for design optimization processes.

CHAPTER 7
CONCLUSION

This study aims to design and develop a vacuum compartment for household refrigerators, intending to decrease the amount of waste food by increasing the food shelf life. The vacuum chamber's design was optimized for the household refrigerators to increase food storage times by storing the foods under low pressure and keep the food at appropriate storage temperatures.

Experimental study and analytical calculations supported by literature research were utilized for determining the design parameters such as types and powers of the components required for the vacuum compartment system design.

An alternative method had to be found for cooling the foods in the vacuum compartment without the forced convection effect. Within this thesis's scope, air channels placed around the compartment, which cooled its walls by the cold air passing through the channels. Subsequently, the internal volume cooling was achieved by radiation effects and natural convection in the low pressure.

Furthermore, with the numerical analysis method performed in this study, the vacuum system design parameters, which are air channel width, refrigerator cooling fan speed and flow guides for homogeneous thermal distribution in the compartment, were selected.

The analysis results show that flow guides succeed the purpose of enhancing the temperature distribution inside the vacuum chamber. However, they dramatically increase the pressure drop; therefore, there are plenty of opportunities to improve them in the aerodynamic sense in further design studies.

As a proof of concept and testing purposes, a concept prototype, designed and manufactured in the light of the system parameters discovered in this study, and this compartment was placed in a household refrigerator. Vacuum compartment cooling tests were performed with this prototype, and the thermal performance of the vacuum chamber was examined. As a result of the thermal tests, it was observed that the refrigerator maintained its temperature with an oscillation between 0 °C and 5 ° C after

it was set to the regime, and the vacuum chamber kept the food in more stable and ideal conditions with a smaller oscillation of 0 °C to 2 °C.

When the thermal test results were compared with the numerical analysis results of the study, it was observed that the average temperature of the vacuum compartment when the refrigerator was set to the regime was similar to the numerical analysis results with an error rate of -0.04%.

As a result of the food tests carried out with the compartment prototype, it was observed that the product storage life increased double times compared to an ordinary refrigerator shelf.

It is hoped that by utilizing and improving the technology and innovation within this thesis, the food shelf lives will enhance more to achieve the most needed reduction in food consumption and contribute to a more sustainable future.

REFERENCES

Acker, R., & Ball, K. M. J. (1977). Modulated vacuum cooling and vacuum treatment of bakery products. *Getreide Mehl Und Brot*, *31*, 134–138.

American Society of Heating, Refrigerating and Air-Conditioning Engineers (2006). *ASHRAE Handbook - Refrigeration*. Atlanta: ASHRAE

Boxer Pumps. (2021). *Boxer 3KD Diaphragm Pump Data Sheet*. Retrieved March 09, 2021, from https://www.boxerpumps.com/en/products/miniature-diaphragm-pumps-air-gas/boxer-3kd-diaphragm-pump-series/

Çengel, Y. A., Boles, M. A., & Kanoglu, M. (2018). *Thermodynamics : an engineering approach* (9th ed.). New York: McGraw-Hill Education.

Chen, Y. L. (1986). Vacuum cooling and its energy use analysis. *Journal of Chinese Agricultural Engineering*, *32*, 43–50.

Chriastel, L. (1978). Acceleration of bread cooling by vacuum. *Prumysl Potravin, 29* (7), 398-401.

Dinçer, I., & Kanoglu, M. (2010). *Refrigeration systems and applications* (2nd ed.). West Sussex: John Wiley & Sons.

Greidanus, P. (1971). Economic aspects of vacuum cooling. *Annual Report of Springier Institute, Wageningen, Netherlands. Project*, *644*, 47–50.

Houška, M., Podloucký, S., Žitný, R., Grée, R., Šesták, J., Dostál, M., et al. (1996). Mathematical model of the vacuum cooling of liquids. *Journal of Food Engineering*, *29* (3), 339–348.

ISO 15502 (International Organization for Standardization 15502). (2005). *Household refrigerating appliance-characteristic and test methods.*

Longmore, A. P. (1973). The pros and cons of vacuum cooling. *Food Industries of South Africa*, *26* (6–7), 9–11.

Malpas, E. W. (1972). Vacuum equipment for evaporative cooling. *Process Biochemistry, 7* (10), 15-20.

Mara, B. K., Mercado, B. C., Mercado, L. A., Pascual, J. M., & Lopez, N. S. (2014). Development and validation of a CFD model using ANSYS CFX for aerodynamics simulation of Magnus wind rotor blades. *2014 International Conference on Humanoid, Nanotechnology, Information Technology, Communication and Control, Environment and Management (HNICEM)*, 1–6.

McDonald, K., & Sun, D.-W. (2000). Vacuum cooling technology for the food processing industry: a review. *Journal of Food Engineering*, *45* (2), 55–65.

McDonald, K., Sun, D.-W., & Kenny, T. (2001). The effect of injection level on the quality of a rapid vacuum cooled cooked beef product. *Journal of Food Engineering*, *47* (2), 139–147.

Miller, R., Miller, M. R., & Anderson, E. P. (2004). *Audel Refrigeration Home and Commercial* (5th ed.). West Sussex: John Wiley & Sons.

Norton, T., & Sun, D.-W. (2006). Computational fluid dynamics (CFD) – an effective and efficient design and analysis tool for the food industry: A review. *Trends in Food Science & Technology*, *17* (11), 600–620.

Omega. (2021). *Omega Thermocouple Types*. Retrieved March 09, 2021, from https://www.omega.com/en-us/resources/thermocouple-types

Shipman, F. P. (1978). Cake technology: interaction between product development and marketing. *Cereal Foods World, 23* (3), 130-131.

Sørensen D. N., D. N. ;Nielsen. (2003). Quality control of computational fluid dynamics in indoor environments. *Indoor Air*, *13* (1), 2–17.

Sun, D.-W. (2001). *Advances in food refrigeration*. Leatherhead: Leatherhead Food Research Association.

Sun, D.-W., & Wang, L. (2000). Heat transfer characteristics of cooked meats using

different cooling methods. *International Journal of Refrigeration*, *23* (7), 508–516.

Sun, D.-W., & Zheng, L. (2006). Vacuum cooling technology for the agri-food industry: Past, present and future. *Journal of Food Engineering*, *77* (2), 203–214.

Tu, J., Yeoh, G.-H., & Liu, C. (2018). Chapter 4 - CFD Mesh Generation. In *Computational Fluid Dynamics A Practical Approach* (3rd ed.) (125–154). New York: Butterworth-Heinemann.

Wang, H., & Zhai, Z. (2012). Analyzing grid independency and numerical viscosity of computational fluid dynamics for indoor environment applications. *Building and Environment*, *52*, 107–118.

Wang, L., & Sun, D.-W. (2002). Modelling vacuum cooling process of cooked meat—part 1: analysis of vacuum cooling system. *International Journal of Refrigeration*, *25* (7), 854–861.

Zheng, L., & Sun, D.-W. (2005). Vacuum Cooling of Foods. In *Emerging technologies for food processing* (2nd ed.) (579–602). Amsterdam: Elsevier